U.S. Department
of Transportation
Federal Railroad
Administration

Safety of High Speed Ground Transportation Systems

Office of Research
and Development
Washington, D.C. 20590

Track Lateral Shift: Fundamentals and State-of-the-Art Review

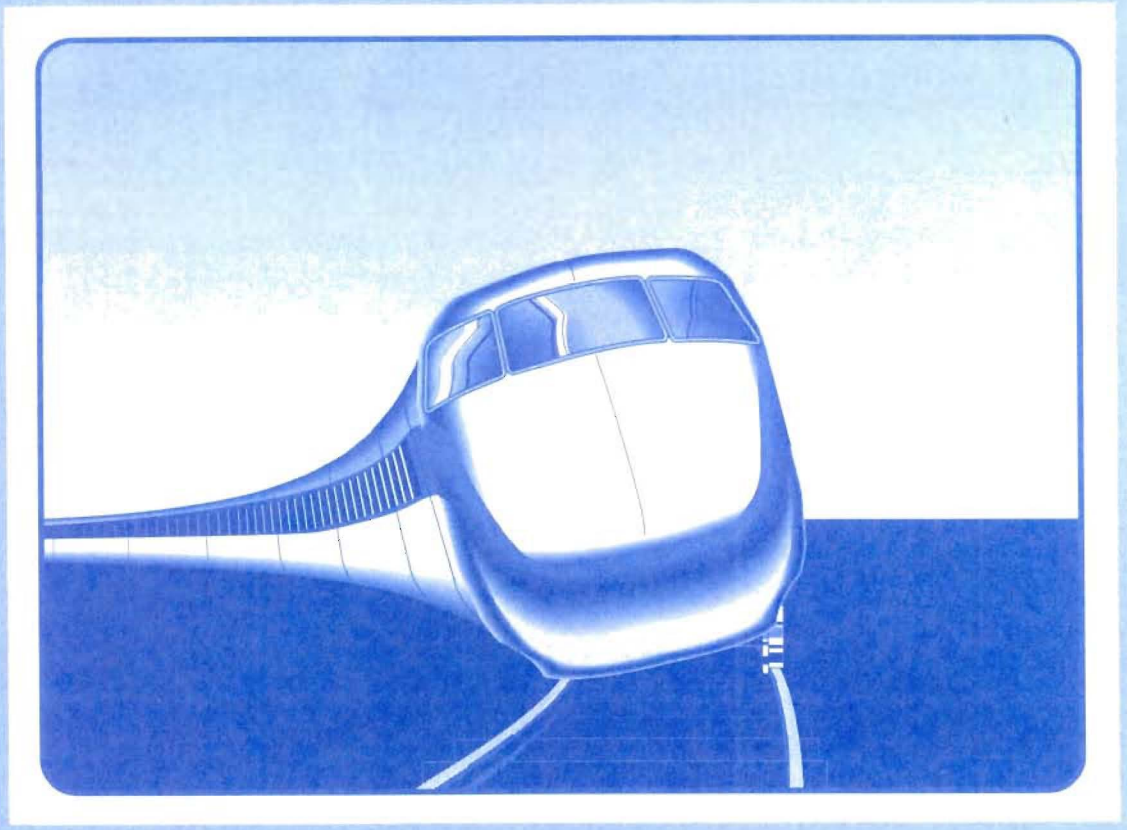

DOT/FRA/ORD-96/03
DOT-VNTSC-FRA-96-1

Final Report
February 1996

REPORT DOCUMENTATION PAGE

Form Approved
OMB No. 0704-0188

1. AGENCY USE ONLY (Leave blank)	2. REPORT DATE	3. REPORT TYPE AND DATES COVERED
	February 1996	Final Report November 1993 - August 1995

4. TITLE AND SUBTITLE
Safety of High Speed Ground Transportation Systems Track Lateral Shift: Fundamentals and State-of-the-Art Review

5. FUNDING NUMBERS
RR593/R5021

6. AUTHOR(S)
G. Samavedam, F. Blader and D. Thomson

7. PERFORMING ORGANIZATION NAME(S) AND ADDRESS(ES)
Foster-Miller, Inc.*
350 Second Avenue
Waltham, MA 02154-1196

8. PERFORMING ORGANIZATION REPORT NUMBER
DOT-VNTSC-FRA-96-1

9. SPONSORING/MONITORING AGENCY NAME(S) AND ADDRESS(ES)
U.S. Department of Transportation
Federal Railroad Administration
Office of Research and Development
400 7th Street, SW
Washington, DC 20590

10. SPONSORING/MONITORING AGENCY REPORT NUMBER
DOT/FRA/ORD-96/03

11. SUPPLEMENTARY NOTES
*under contract to:
U.S. Department of Transportation
Research and Special Program Administration
John A. Volpe National Transportation Systems Center
Cambridge, MA 02142

12a. DISTRIBUTION/AVAILABILITY STATEMENT
This document is available to the public through the National Technical Information Service, Springfield, VA 22161

12b. DISTRIBUTION CODE

13. ABSTRACT (Maximum 200 words)

This report presents a review of the state of the art of track lateral shift analysis, with improved concepts for safety evaluation of high speed trains generating track shift forces.

The mechanics of track shift and the resulting track failure modes are defined. A critical review of the track shift literature from France, England, Sweden, Japan and the United States is presented. The review reveals that the French National Railways (SNCF) has developed an in-depth understanding of the technical issues in track shift. The SNCF work identified the stable and progressive track shift phenomena due to high speed vehicle passage on curves and tangent tracks with misalignments. Track shift safety criteria, which are specific to their high speed operations, were experimentally developed.

An approach is suggested in this report for an improved understanding and analysis of track shift for application to the U.S. track conditions. The proposed approach consists of a vehicle dynamic model to predict lateral loads on the track, and a track model to determine limit loads on the track and residual lateral deflections under the influence of the vehicle loads. The model can also evaluate the ride quality and potential for wheel climb derailment. The vehicle dynamic model is based on a lumped mass system, and maintains a rolling contact mechanism between the wheel and the rail. Preliminary numerical results are presented to demonstrate the applicability of the model in the study of track shift.

The track model framework presented uses fundamental track parameters including the tie-ballast lateral resistance. Using the model, preliminary results are presented on the track limiting strength. A basis on which residual deflections of track under vehicle passage are quantified is also indicated. The proposed models will be fully developed in the next phase of this study.

14. SUBJECT TERMS	15. NUMBER OF PAGES
Track lateral shift, high speed rail, track/vehicle analysis, track panel shift	76
	16. PRICE CODE

17. SECURITY CLASSIFICATION OF REPORT	18. SECURITY CLASSIFICATION OF THIS PAGE	19. SECURITY CLASSIFICATION OF ABSTRACT	20. LIMITATION OF ABSTRACT
Unclassified	Unclassified	Unclassified	

PREFACE

This report presents a comprehensive review of the state of the art of track shift, and advanced concepts for safety evaluation of high speed trains generating track shift forces. This work has been performed under the OMNI contract DTRS-57-93-D00028 awarded by the Volpe National Transportation Systems Center (VNTSC), at Cambridge, MA. The work was performed by Foster-Miller, Inc. under the technical direction of Dr. Andrew Kish, the Technical Task Initiator of VNTSC. The work was sponsored by the Office of Research and Development, Federal Railroad Administration, U.S. Department of Transportation at Washington, D.C. Mr. William Paxton of FRA was in charge of this research program.

The authors are grateful to Dr. David Wormley for his comments and inputs during the performance of this work. The authors also wish to thank Dr. Herbert Weinstock of VNTSC for his comments on an earlier version of this document.

METRIC/ENGLISH CONVERSION FACTORS

ENGLISH TO METRIC

LENGTH (APPROXIMATE)

1 inch (in)	=	2.5 centimeters (cm)
1 foot (ft)	=	30 centimeters (cm)
1 yard (yd)	=	0.9 meter (m)
1 mile (mi)	=	1.6 kilometers (km)

AREA (APPROXIMATE)

1 square inch (sq in, in^2)	=	6.5 square centimeters (cm^2)
1 square foot (sq ft, ft^2)	=	0.09 square meter (m^2)
1 square yard (sq yd, yd^2)	=	0.8 square meter (m^2)
1 square mile (sq mi, mi^2)	=	2.6 square kilometers (km^2)
1 acre = 0.4 hectare (he)	=	4,000 square meters (m^2)

MASS - WEIGHT (APPROXIMATE)

1 ounce (oz)	=	28 grams (gm)
1 pound (lb)	=	0.45 kilogram (kg)
1 short ton = 2,000 pounds (lb)	=	0.9 tonne (t)

VOLUME (APPROXIMATE)

1 teaspoon (tsp)	=	5 milliliters (ml)
1 tablespoon (tbsp)	=	15 milliliters (ml)
1 fluid ounce (fl oz)	=	30 milliliters (ml)
1 cup (c)	=	0.24 liter (l)
1 pint (pt)	=	0.47 liter (l)
1 quart (qt)	=	0.96 liter (l)
1 gallon (gal)	=	3.8 liters (l)
1 cubic foot (cu ft, ft^3)	=	0.03 cubic meter (m^3)
1 cubic yard (cu yd, yd^3)	=	0.76 cubic meter (m^3)

TEMPERATURE (EXACT)

[(x-32)(5/9)] °F = y °C

METRIC TO ENGLISH

LENGTH (APPROXIMATE)

1 millimeter (mm)	0.04 inch (in)
1 centimeter (cm)	0.4 inch (in)
1 meter (m)	3.3 feet (ft)
1 meter (m)	1.1 yards (yd)
1 kilometer (k)	0.6 mile (mi)

AREA (APPROXIMATE)

1 square centimeter (cm^2)	0.16 square inch (sq in, in^2)
1 square meter (m^2)	1.2 square yards (sq yd, yd^2)
1 square kilometer (km^2)	0.4 square mile (sq mi, mi^2)
10,000 square meters (m^2)	1 hectare (he) = 2.5 acres

MASS - WEIGHT (APPROXIMATE)

1 gram (gm)	0.036 ounce (oz)
1 kilogram (kg)	2.2 pounds (lb)
1 tonne (t) = 1,000 kilograms (kg)	1.1 short tons

VOLUME (APPROXIMATE)

1 milliliter (ml)	0.03 fluid ounce (fl oz)
1 liter (l)	2.1 pints (pt)
1 liter (l)	1.06 quarts (qt)
1 liter (l)	0.26 gallon (gal)
1 cubic meter (m^3)	36 cubic feet (cu ft, ft^3)
1 cubic meter (m^3)	1.3 cubic yards (cu yd, yd^3)

TEMPERATURE (EXACT)

[(9/5) y + 32] °C = x °F

QUICK INCH - CENTIMETER LENGTH CONVERSION

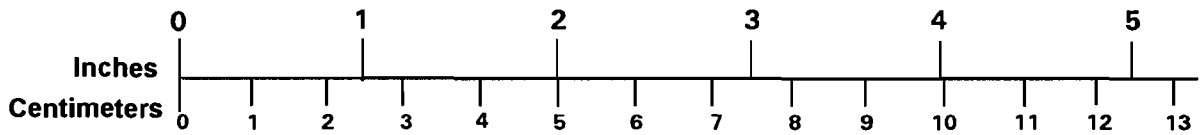

QUICK FAHRENHEIT - CELSIUS TEMPERATURE CONVERSION

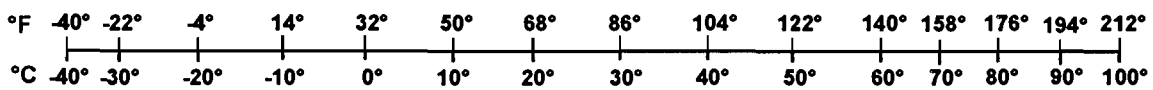

For more exact and or other conversion factors, see NBS Miscellaneous Publication 286, Units of Weights and Measures.
Price $2.50 SD Catalog No. C13 10286

Updated 1/23/95

TABLE OF CONTENTS

Section **Page**

LIST OF ILLUSTRATIONS

Figure **Page**

LIST OF TABLES

LIST OF SYMBOLS

A	Cross-sectional area for two rails
E	Young's modulus for rail steel
$\bar{F}$	Nonlinear part of track lateral resistance accounting for softening
F_{base}	Track lateral resistance due to tie base friction
F_L	Track limiting lateral resistance
F_p	Track peak lateral resistance
$F_{p,d}$	Track dynamic peak lateral resistance
$F_{p,s}$	Track static peak lateral resistance
H	Net lateral load exerted on the track by the vehicle axle
H_p	Prud'homme limit for lateral force
I	Moment of inertia for bending in the lateral plane (2 rails)
I_v	Moment of inertia for bending in the vertical plane (2 rails)
k_v	Track foundation vertical stiffness
L	Track lateral deflection half-wavelength
L/V	Ratio of lateral to vertical forces (as defined on page 26)
N	Number of vehicle passes
P_o	Track thermal force
Q	Track self-weight
R	Track radius of curvature
R_v	Track foundation vertical reaction
S	Ballast reaction in the lateral plane
S_d	Track lateral dynamic strength under moving load
S_s	Track lateral strength under stationary load

S_l	Track lateral limiting static strength under stationary load
ΔT	Rail temperature increase above neutral
V	Vehicle vertical axle load
w	Track lateral deflection
w_L	Tie deflection at its limiting resistance
w_p	Tie deflection at its peak resistance
$\bar{\delta}$	Initial misalignment after realignment or construction
δ_c	Critical track lateral misalignment
δ_m	Maximum allowable premaintenance misalignment
δ_s	Stable track shift misalignment
μ_f	Tie-ballast coefficient of friction

EXECUTIVE SUMMARY

Track lateral shift under high speed vehicle lateral loads is an important phenomenon influencing the safety of the high speed ground transportation systems. The lateral shift can be gradual with the passage of vehicle traffic or sudden if the track lateral strength is inadequate. Potential failure modes resulting from the track shift include catastrophic track buckling, derailment due to wheel climb or gage widening, and ride quality deterioration.

In this report, the fundamental mechanics of the track shift phenomenon are presented in detail, identifying the critical conditions for the failure modes originating from the track shift. A comprehensive review of the literature published in France, England, Sweden, Japan and the United States is presented. The track shift criteria practiced in these countries are critically examined. It is concluded that despite the good research work done by the French National Railways (SNCF) in the last few decades, the state of the art remained empirical. The lack of a rigorous analysis of the track shift phenomenon makes it difficult and questionable to adopt the empirical criteria of the foreign railroads for U.S. railroads, particularly due to the wide range in construction and maintenance practices as well as operating environment.

A rational approach for analyzing track shift under vehicle and thermal loads is outlined. The approach consists of using a vehicle dynamic model to determine lateral loads generated on the track, and a track model to evaluate the track lateral response and the resulting residual deflections after the vehicle passage.

Vehicle dynamic computer codes (such as SYSSIM) exist and can be further improved to include track compliance. At present, there is no adequate track model that can give track shift residual deflections. An approach is suggested for the development of such a track model.

Preliminary numerical results on lateral loads are presented using the SYSSIM vehicle dynamic code. A TGV-type vehicle consist is simulated for this purpose. Baseline results on limiting track strength are also presented using a simplified track model.

Conclusions of practical interest based on the literature survey conducted are presented. Recommendations for improved vehicle and track models for track shift evaluations are also made.

1. INTRODUCTION

European and Japanese railroads have developed and operated high speed rail systems for some time. Track shift has been recognized as an important safety and operational issue for these railroads. The French National Railways (SNCF) has had an active research program in this area for the last three decades. Other railroads such as German Railways (DB), British Rail (BR) and Sweden Railways (SJ) have also started major research programs on testing and analyses of track shift.

With the expected introduction of high speed rail systems in the near future in the United States, and for purposes of comparison of high speed rail with other modes of transportation, there is a need to evaluate the safety and efficiency of high speed rail in the United States. The Federal Railroad Administration (FRA) has sponsored research on track shift through the Volpe Center's (VNTSC) technical support.

The first milestone in the Track Shift Research Program is a state-of-the-art review of the literature. Foster-Miller has completed this review study, the results of which are contained in this report.

Section 2 of this report first addresses the basic definition of track shift and the key safety issues related to this phenomenon. It identifies track shift as the growth of the lateral misalignment from the initial value at the time of track construction or after realigning operations. Four major failures of track structure and vehicle operations which originate from the lateral misalignments are identified. These are: 1) sudden track shift, 2) track buckling, 3) ride quality deterioration; and 4) derailment due to wheel climb or gauge widening. In addition, the misalignment may itself cause the vehicle to exceed lateral design loads. Critical track shift conditions can be expressed in terms of lateral deflection, vehicle loads and track lateral strength. The premaintenance track misalignment amplitude is also introduced as a parameter in the track shift studies.

Section 3 presents a critical review of the available literature on track shift in France, England, Germany, Sweden and the United States. Work done by the railroad organizations in these countries and also by the Union of International Railways (UIC/ORE) is examined. The review showed that there is widespread usage of the Prud'homme criterion as a guideline for vehicle qualification. A track shift criterion has been developed by SNCF; however, there is no general agreement on this track shift criterion. The review also indicated that the SNCF approach is essentially based on vehicle tests on specific track conditions, and their data have not been correlated theoretically or in terms of basic track parameters. Hence, it is not appropriate to use their track shift data for U.S. track conditions.

Section 4 presents the vehicle modeling requirements for an assessment of vehicle loads, and track misalignment levels for potential derailment and reduced ride quality beyond the required limits. The SYSSIM code now in use at Foster-Miller has been exercised on a TGV-type consist, and some data on critical track misalignments are presented. The model needs to be improved in its track structure simulation to enable a more accurate assessment. SYSSIM will thus form an important tool for further development in the track shift studies.

Section 5 gives the requirements of a track structure model for track shift quantification. Important track parameters, including the loaded tie-ballast resistance, are identified. The problem of determining the loaded track panel response and its residual deflections under loading and unloading cycles is addressed. A theoretical approach is outlined to determine the cumulative track residual deflection due to vehicle passes. This will determine the track strength requirements for stabilization under a finite number of passes. The analysis procedure will also determine the critical track shift conditions producing a sudden or rapid increase in misalignment growth under a limited number of vehicle passes.

Basic track panel test requirements under repeated static loads are also presented for the validation of the theoretical model and preliminary assessment of track shift.

Section 6 presents significant conclusions of the present state-of-the-art survey and recommendations on the short-term need of the track shift research in the United States.

2. TRACK SHIFT FUNDAMENTALS

In this section the background and the mechanics of track shift and related track failure modes are presented.

Both jointed and continuous welded rail (CWR) tracks may experience deviations in lateral alignment under revenue operations. Several causes can be attributed to this phenomenon, the primary factor being the vehicle loads. Vehicle lateral loads tend to move the track laterally, whereas the vertical loads tend to stabilize the track by increasing the frictional resistance at the tie bottom. In CWR track, the thermal load also plays a significant role.

Track shift is defined as the permanent lateral distortion of a track segment, which can occur under vehicle passes due to resulting lateral loads and which can lead to unsafe conditions for further traffic unless remedial maintenance actions are taken. The permanent lateral distortion can occur cumulatively under vehicle passes, or can occur suddenly under a single or a number of passes.

Track shift can occur locally or can be spread over a long section of track. The latter is caused in weak curved tracks when a steady curving force is exerted by the vehicles. The local shift is caused by vehicles negotiating a pre-existing irregularity. Track shift can also be caused by loads resulting from vehicle hunting. Radial movement of curves under thermal loads is another example of track shift.

Studies on track shift are required for the following reasons:

- In the design and maintenance of modern high speed track, adequate track lateral strength must be assured to withstand vehicle and thermal loads. Track shift potential is the ultimate consideration in determining the required lateral strength.

- Track shift should be eliminated or controlled to occur at a slow rate (with respect to the traffic tonnage) so that periodic track inspection, realignment and other maintenance operations can be planned in an economical manner, particularly for high speed tracks.

- Track shifting forces can be a major contributor to the formation and growth of local track geometric imperfections. Vehicle operators must know the allowable track shifting forces to limit vehicle loads and speeds. Therefore, vehicle qualification tests should be performed on tracks with known and prescribed lateral strength. Although empirical guidelines exist on vehicle qualification loads, they may be too conservative or in some cases nonconservative as discussed later in this report.

- For corridors such as the Northeast, where tracks (with curvatures and high superelevations) already exist, it is necessary to define the maximum safe speeds for high speed train operations. Although the speed limits for conventional vehicles are decided from considerations of ride comfort, wheel climb derailment potential, and other

safety considerations, new emerging vehicles such as the X2000 can overcome some of these limits. To achieve higher speeds than permitted for the conventional vehicle, the ultimate limit may be based on track shift considerations.

In summary, it is important to define the ultimate track lateral strength for planning safe vehicle operations and the evaluation of vehicle qualification loads.

2.1 Track Strength Definition

Referring to Figure 2-1, the track shifting forces include the vehicle net axle lateral loads, H, and the thermal compressive loads, P_0, in the rail. The net axle loads include the curving force and the dynamic augment due to any initial misalignment. The vehicle and thermal loads are reacted by the ballast (friction on the tie bottom, sides in the ballast crib and the ballast shoulder at the tie ends). The resultant ballast reaction in the lateral plane is schematically represented by S. Under dynamic equilibrium conditions, there will be a resulting track lateral dynamic deflection, which may not vanish (i.e., the track may not completely recover its initial configuration) after the vehicle passage. This is due to the "elasto-plastic" characteristic of the ballast discussed in Section 5. Hence, there can be a permanent or residual deflection of the track structure. Under certain conditions, the permanent deflection can accumulate globally (in the case of curved tracks) or locally at weak spots such as misalignments (in the case of tangent tracks). Clearly, if the vehicle load exceeds the maximum reaction that can be offered by the track panel, then the resulting track deflection can be rapid and excessive for safe operations of vehicles. The maximum resistance that can be offered by the track to moving loads without excessive residual deflections will be called the track "dynamic" strength, S_d.

The track dynamic lateral strength, S_d, must be distinguished from its static lateral strength, S_s, which is the maximum stationary load that can be sustained by the track without excessive permanent deflections. The dynamic strength is for an indefinite number of axle passes whereas the static strength is for many cyclic load applications at the stationary load point. Clearly, it is important to define the allowable residual deflections in the evaluation of static or dynamic strengths. This will be determined from considerations of safety, of track and

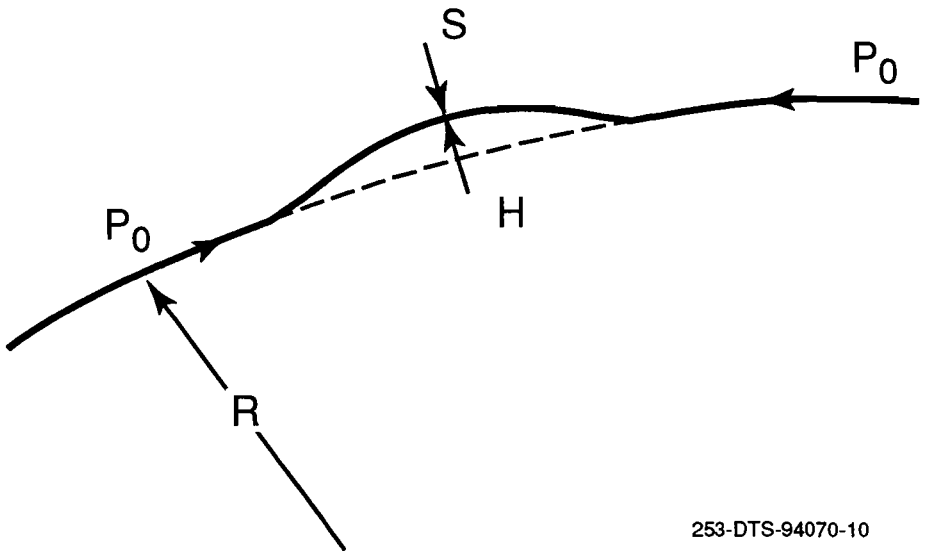

Figure 2-1. Track shifting forces and track reaction definition

vehicle operations, and will be a subject of future investigations. It is important to recognize that the dynamic lateral strength is significantly less than the static strength. This has been demonstrated in the SNCF tests on track shift, and will be analytically investigated in a forthcoming report.

The French have determined track dynamic strength experimentally by applying a known moving lateral load on tracks through a single axle under vertical load. The axle is situated sufficiently far away from other axles to minimize interference on the vertical load distribution. The vehicle runs at slow speed. After the passage of the vehicle over the test segment, the mean transverse residual displacement is measured. The lateral load is incremented at each pass. The relationship between the applied axle lateral load and the residual deflection is typically as shown by the full line in Figure 2-2. The load at which significant residual deflection begins to occur was originally considered as the track dynamic strength. This definition was later refined on the basis of tests with multiple passes at constant lateral axle force. The typical data is shown in Figure 2-3 which relates the track shift to the number of passes. These curves show that for values of lateral force below a limit, the track deflections *stabilize* at some finite value. Above this critical lateral force, the deflection is found to increase at a very rapid rate. The lateral load below which the deflections stabilize at permissible values will be defined here as the track dynamic lateral strength. Thus, referring to Figure 2-3, H_1 will be regarded as dynamic strength and not H_2, since the deflection at H_2 stabilizes at a value higher than the permissible (δ_m).

This dynamic track strength is a complex function of the track parameters which are discussed in Section 5.

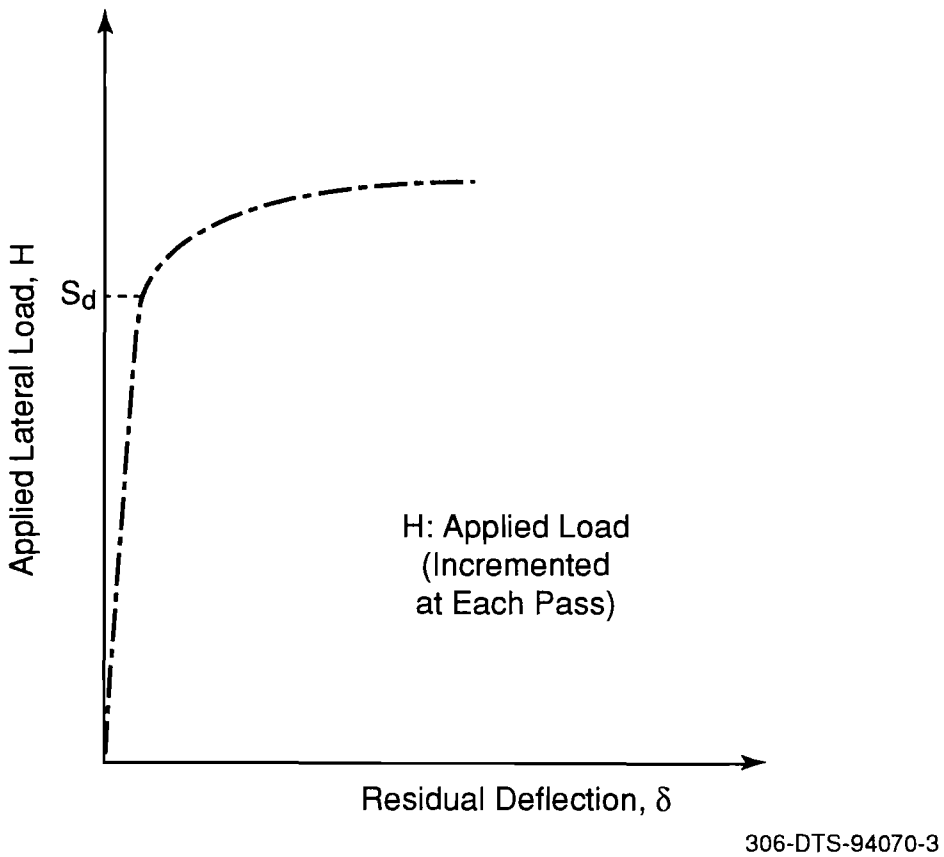

Figure 2-2. Track shift versus net axle load

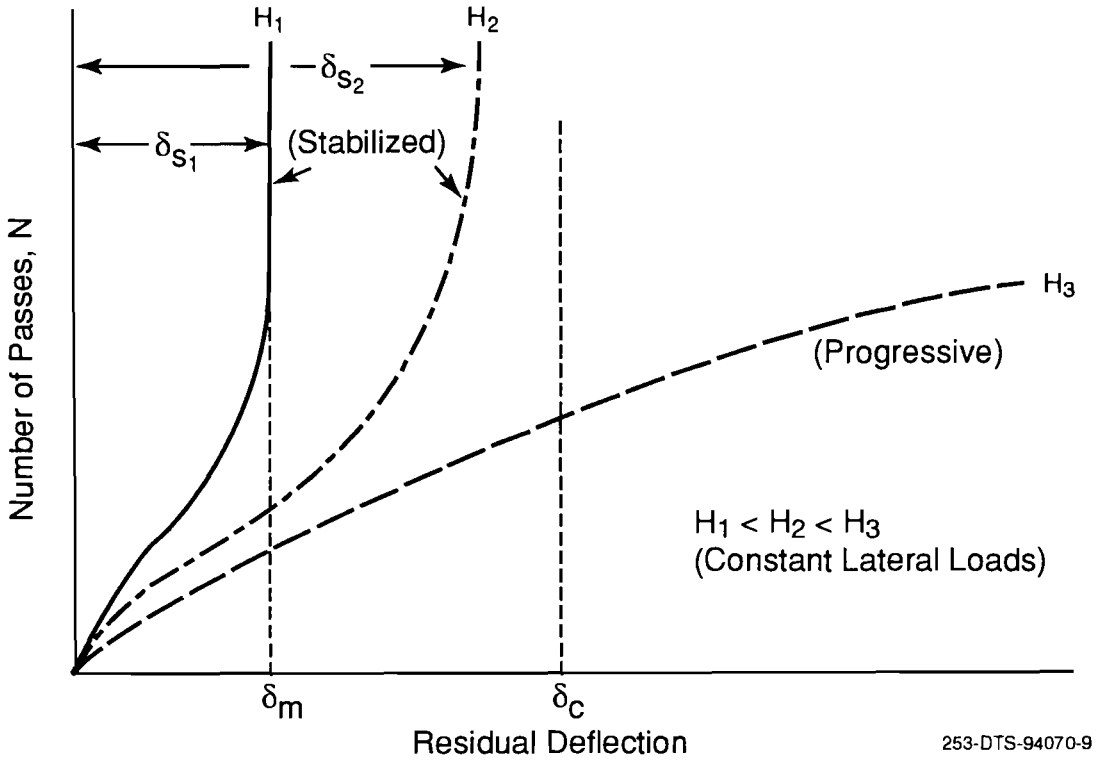

Figure 2-3. Track shift versus vehicle passes (Definition of dynamic strength)

2.2 Allowable Misalignments and Track Shift

From Figure 2-3, it is seen that track shift itself is a form of misalignment for subsequent traffic even though it may reach a stable level. For high speed traffic, four levels of lateral misalignment are important as recognized by the European researchers. These are:

- Initial misalignment after realignment or construction, $\bar{\delta}$.
- Maximum allowable premaintenance misalignment, δ_m.
- Critical misalignment at which operations are impacted, δ_c.
- Stable track shift misalignment levels reached after many passes, δ_s.

The initial misalignment after realignment or construction tolerance for new tracks is represented by $\bar{\delta}$. This misalignment may be on the order of one or more millimeters for high speed tracks.

The maximum allowable misalignment prior to maintenance operations according to the individual railroad practices is represented by δ_m. For example, the SNCF uses about 4 mm as the maximum limit for their TGV track maintenance.

The critical misalignment amplitude at which vehicle operations are impacted or where track structure fails is represented by δ_c. Several possible failure modes may have to be considered to determine the lowest value of δ_c. These are discussed in the following subsection. As discussed later in Section 3, reference (11), the SNCF indicates 12 mm peak to

peak as a possible value of δ_c for their TGV track, at which the track is not considered to be traffic worthy. Mere realignment is not considered to be adequate at this misalignment level. Additional work involving ballast consolidation and packing is required.

The displacement δ_s in Figure 2-3 is the stable deflection at a large number of passes and is clearly reached only if δ_c, the critical misalignment, is larger than δ_s. For low speed track, δ_s can be on the order of 20 mm according to published test data, and δ_c can be larger than that. For high speed track, stabilization may not be reached prior to the critical misalignment limit, δ_c. *It is important to determine δ_c, the critical misalignment, for high speed tracks, and evaluate the risk involved in the choice of δ_m by railroad practices.*

The critical misalignment δ_c, can be determined from mechanistic considerations for given vehicle parameters, speed and track resistance characteristics, although at present there is no suitable theoretical model to do this. The premaintenance misalignment, δ_m, can be derived on a tradeoff between the frequency of maintenance (number of safe vehicle passes or MGT) and the margin of safety based on the critical misalignment, δ_c. The construction tolerance, $\bar{\delta}$, is usually determined by the railroads as a tradeoff between the cost of construction, maintenance and the number of revenue passes that can be obtained between maintenance cycles.

Although there is no explicit discussion on the wavelengths associated with the misalignments, the wavelengths are of interest in the track shift analysis. The wavelength associated with the construction tolerance is on the order of a few meters. For δ_m, it can be in the range of 10 to 20m for typical high speed track. For δ_c, the wavelength can be in the range of 20 to 40m.

2.3 Critical Track Conditions

The critical track conditions are defined by the critical misalignment and the critical vehicle lateral loads. Additional vehicle passes after the critical limits are reached can lead to one or more of the following failure modes some of which are illustrated in Figure 2-4.

1. *Sudden Track Shift Potential* - In combination of the increased vehicle loads, and the thermal loads, sudden track shift (of the order of 20 to 40 mm) can occur, particularly for curved tracks or in the presence of the misalignment. Alternately, the overall track panel resistance, S, may be inadequate to resist the vehicle loads, which will result in a rapid increase in residual deflections under additional passes, leaving an insignificant safety margin.

2. *Derailment* - The critical conditions can lead into wheel climb or other derailment failures. Rail rollover and gauge widening are also possibilities.

3. *Buckling* - The combination of critical misalignment and the rail thermal loads can lead to CWR track buckling (or a reduction of the buckling safety margin) due to the loss of lateral resistance in the uplift zone in-between the trucks. This mode of failure can generate large levels of track movement, on the order of several centimeters.

4. *Reduced Fatigue Life* - Vehicle lateral loads can exceed the values, for which the vehicle suspension and other parameters are designed. This can reduce the vehicle component fatigue life significantly, or restrict the safe operating speed.

5. *Inadequate Ride Quality* - At high speeds, the critical imperfection can be such as to yield lateral jolts or high lateral accelerations exceeding the tolerable limits of ride quality.

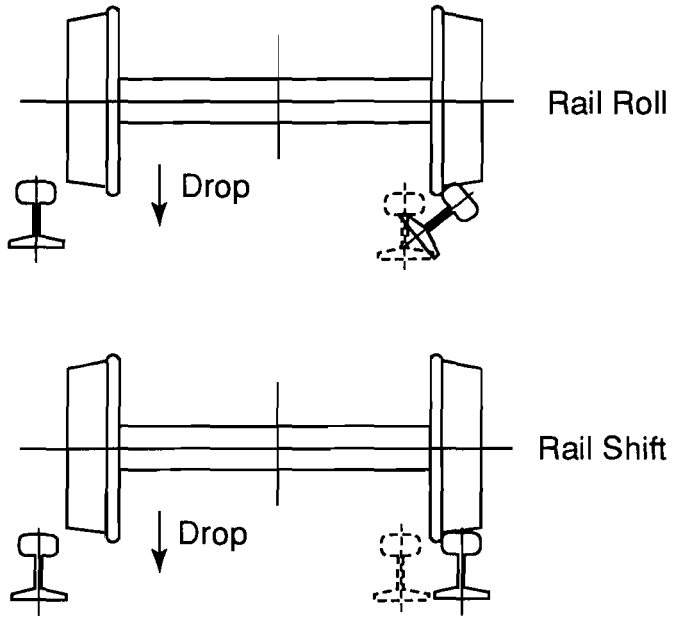

Figure 2-4. Failure modes

2.4 Track Shift Criterion

The track shift criterion to be developed in this program should be distinguished from the vehicle acceptance criterion. The latter encompasses both performance and safety to cover a range of vehicle operations over a range of track conditions. The track shift criterion will provide a detailed evaluation of safety and track degradation in the lateral plane on track segments with known parameters, under known net axle loads.

The early Prud'homme formula (1) based on track shift issues became a vehicle acceptance criterion in some of the European railroads. Prud'homme, of course, was aware of the difference in the two criteria, but synthesized the two criteria by introducing a "reference track." In the United States, no reference track exists as yet although the present FRA classification defines the geometry limits for tracks. The lack of prescribed minimum lateral strength limits for U.S. tracks makes it difficult, at present, to use a simple track shift criterion as a component in the overall vehicle acceptance criterion.

The key elements involved in the analysis of track lateral shift are summarized in Figure 2-5. If we assume that a high speed vehicle with known characteristics is available for revenue operations on U.S. tracks, then the pertinent questions on track/vehicle safety are:

- What is the minimum track strength required for normal (full speed) operations of the vehicle?

- What is the critical misalignment, δ_c, at which operations are unsafe?

- What is the maximum permissible premaintenance misalignment, δ_m, which will give maximum flexibility for the railroads? What is the margin of safety involved before the critical condition δ_c is reached?

These questions can be answered through a systematic analysis and test validation program. The results of this program can be condensed into a Track Shift Safety Criterion for use by the industry. The criterion can be expressed in one or more of the following forms:

- The track under extreme thermal loads should, for a given vehicle, have a minimum lateral strength to limit the growth rate of lateral imperfections to under a specified value.

- The cumulative growth of lateral irregularity permissible under normal operations should have a factor of safety of (say) 2, over the critical growth level, δ_c, at which the vehicle and track will be unsafe for revenue operations.

- The lateral loads generated by high speed vehicles under the extreme permissible track irregularity should not exceed the lateral dynamic track strength under extreme thermal loads.

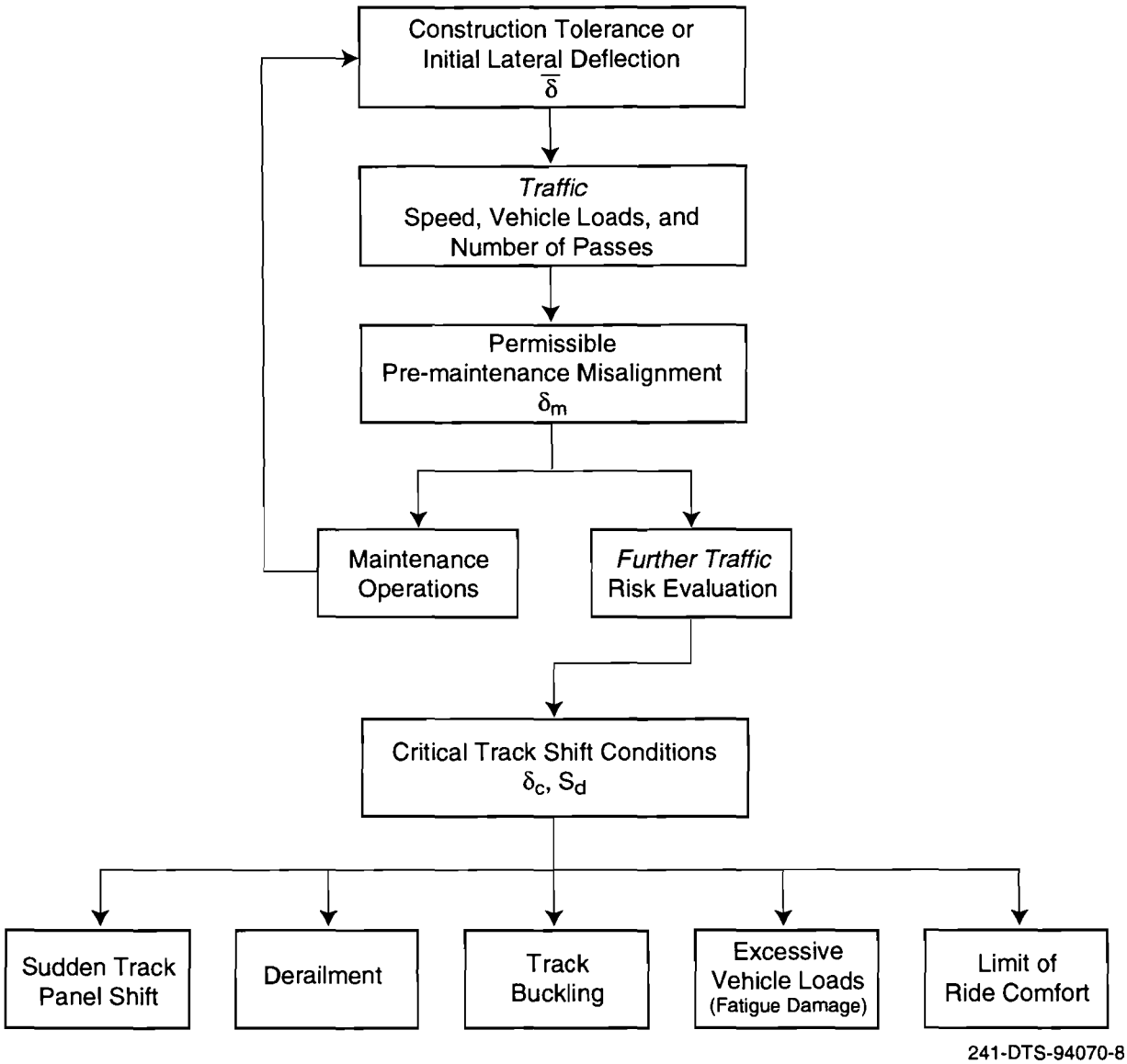

Figure 2-5. Safety aspects of track shift

3. CRITICAL REVIEW OF THE LITERATURE

The available literature on track shift including analytical and experimental works as well as the practices followed or recommended by the railroad organizations is reviewed here. The literature review includes work done in France, Great Britain, Germany, Sweden and Japan, as well as in the United States.

The mechanisms involved in track shift phenomena are complex, and are influenced by such factors as vehicle dynamic loads, track ballast and tie types, track misalignments and thermal loads. To date, very limited experimental data and analyses are available to guide operating criteria. The most extensive work has been conducted in Europe to develop initial guidelines based on relatively simple models and limited tests. In this section, the test and analytic data will be reviewed and research needs for improved understanding of track shift will be pointed out. For consistency in the following sections, as was shown in Figure 2-1, H will be used to represent the vehicle load (specifically the net axle lateral load); S will designate the equivalent ballast reaction, and S_d the limiting track panel strength.

3.1 SNCF/ORE Studies

The SNCF has been the most significant contributor to the subject of track shift. This subject has evolved over the last three decades of intense research, starting with the historical work by Prud'homme, who experimentally evaluated the lateral strength of a wood tie track under a moving lateral load. The ORE embarked on a major research program in recent times to quantify the lateral strength of modern tracks which will be discussed later in detail.

3.1.1 SNCF Analyses

Prud'homme (1) developed the first empirical equation for the lateral strength of a wood tie track under vertical axle loads. Over the years, this equation has served as a guideline for vehicle qualification loads. Therefore, consistent with the terminology in this report, the Prud'homme limit will be represented by H_p as follows:

$$H_p = 10 + V/3 \text{ kN}, \tag{3-1}$$

where

V = vertical axle load.

This empirical criterion originally defined the limiting track panel resistance of a wood tie track with tamped macadam ballast required to prevent or minimize track shift under repeated loads. This formula did not account for the curvature and the rail thermal load effects. Prud'homme later recommended a multiplying factor of 0.85 to H_p for these effects. This is known as 85 percent of the Prud'homme limit.

Amans and Sauvage (2) developed a theoretical analysis for the loaded track panel response. On the basis of the theory, they developed an expression for the limits on vehicle loads which ensures that the track shift occurs only at a "very slow rate" with respect to the

number of vehicle passes. This slow progression of track shift will facilitate track inspection and maintenance.

Amans and Sauvage (2) developed the following relationship for allowable vehicle loads.

$$H = \rho\left[10 + \frac{V}{3}\right](kN) \tag{3-2}$$

where the quantity ρ, defined below, is used to reflect the influence of rail temperature, track curvature and track geometric and material properties on the panel resistance:

$$\rho = \left[1 - 0.125\,AT\left(1 + \frac{800}{R}\right)\right]\left(\frac{k_v}{2x10^7}\right)^{1/8} 0.225\,\frac{(EI)^{1/4}}{(EI_v)^{1/8}} \tag{3-3}$$

where:

R = radius of the curve (m).

T = increase in temperature of the rails above the neutral temperature (°C).

EI = bending rigidity of the two rails in the transverse direction (Nm^2).

EI_v = bending rigidity of the two rails in the vertical direction (Nm^2).

A = rail section (m^2).

k_v = foundation modulus of the track (N/m^2).

This relationship for ρ was essentially developed on a theoretical basis. The influence of some of the parameters appears to be minimal according to the numerical results given by Kish (3). For extreme examples, a 40°C (72°F) temperature differential results in only a 6 percent decrease in H and a 12 deg curve with a 20°C (36°F) temperature differential results in only a 10 percent decrease in the allowable load.

The SNCF theoretical work which provided a basis for understanding the track shift phenomenon can be improved to incorporate the following features:

- Express the track lateral strength in terms of the basic track parameters such as the unloaded ballast resistance, tie-ballast friction coefficient and others as discussed in Section 5.
- Account rigorously for the influence of curvature and thermal load.
- Include the effect of track misalignments in the generation of dynamic loads and the influence of these loads on the growth of imperfections, in addition to the influences of steady loads.
- Study the influence of multiple axle loads on the track shift.

3.1.2 SNCF/ORE Tests

Original SNCF Tests

The Prud'homme tests were conducted at Vitry-sur-Seine on U33 (46 kg/m) CWR track with wood ties spaced at 0.58m and RNS clamps. The test track had a curvature of 2.2 deg (800m radius) and was new with no traffic consolidation. Joule heating was utilized to increase the longitudinal thermal stresses in the rail. Two test loading vehicle designs were utilized. The first design was a single "derailleur" vehicle with an 8.2m (27 ft) wheelbase and a center active axle capable of applying a maximum vertical load of 120 kN (27 kips) and a maximum lateral load of 110 kN (25 kips). The second design, designated the wagon "tombereau," consisted of two coupled vehicles on parallel tracks. One vehicle propelled the other vehicle and applied a lateral load to one of its axles. The maximum loads for this design were 130 kN (29 kips) vertical and 170 kN (38 kips) lateral. The results from the two designs were apparently similar.

Two test methodologies were used by the SNCF. The following load parameters were used.

- Method 1: Vertical load constant, lateral load incremented after every pass or after every ten passes.
- Method 2: Both vertical and lateral load kept constant at all passes.

Using Method 1, the cumulative residual deflection was obtained as a function of the lateral load. Figure 3-1(a) shows the test data obtained for three different applied vertical load levels. Ten passes were made at each lateral load level in this case. Both the total deflection, that which is recorded while under load, and the residual deflection, that which remains after load

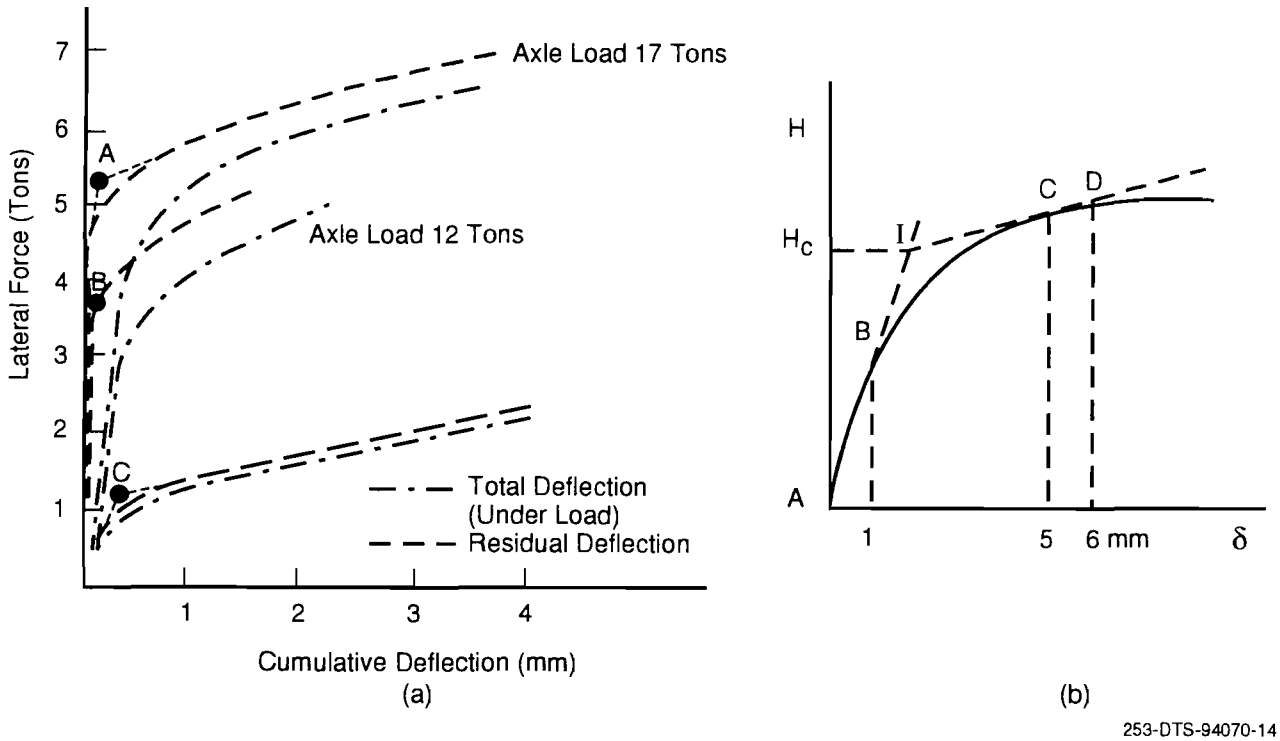

Figure 3-1. Lateral resistance and deformation of loaded track (4)

is removed, are shown. The critical load has been defined by different researchers through numerous empirically derived criteria. For tests where one pass was made at each load level, this critical load was defined by the empirical procedure indicated in Figure 3-1(b). In this method, two lines are constructed. One line passes through the origin (point A) and the 1 mm deflection point (point B) on the load deflection curve. The second line passes through the 5 mm and 6 mm deflection points (points C and D) on the load deflection curve. The critical load is defined at the intersection of the two constructed lines (point I). For tests such as those shown in Figure 3-1(a), where ten passes were made at each load level, two target lines were constructed against the nearly bilinear load deflection curve. The intersection of these lines then defined the critical load. Thus, the critical lateral loads for each of the three vertical load levels are designated by points A, B, and C in Figure 3-1(a) based on the residual deflection.

Using Method 2, the SNCF obtained a relationship between the residual deflection and a larger number of passes. At certain load combinations, the deflection was found to be "stable." Stable track conditions, according to the SNCF, seem to represent decreasing incremental growth of deflection with a finite number of passes. For other load combinations, the deflection increased rapidly without reaching any stable limits. The transition between the stable and the unstable deflection growth was determined to be representative of critical conditions.

The SNCF test methodology provided a valuable approach to the track shift phenomenon which is expressed in terms of the track residual deflection as a function of the lateral axle load and the number of vehicle passes. Stable and unstable regimes of the residual deflections are identified. The following additional studies are desirable for improved understanding of track shift and application of the test data to the track maintenance.

- The transition between the stable and unstable regimes should be clearly determined.
- The residual deflection may stabilize at a considerable deflection which may not be safe for revenue operations. It is desirable to quantify the growth rate of residual deflections at a given lateral load for planning track maintenance.
- Tests simulating multiple axle loads will be useful in establishing the adequacy of the single axle load used in the SNCF work.
- Constant lateral loads simulated the steady vehicle curving forces. Loads generated by vehicle-track interaction (hunting forces, dynamic loads generated at lateral misalignments) and their influence on track shift should also be experimentally determined.

SNCF Tests of TGV Track

Later tests were conducted by the SNCF on the TGV Paris-South-East line near Tonnere (5) primarily to measure the panel resistance for the new track design and to compare this resistance with previous SNCF experiments conducted on older track. These tests are particularly significant in the development of a resistance characterization methodology in that a specific criteria for the definition of the limiting lateral resistance is provided.

Tests were conducted using the "derailleur" wagon which applied vertical and lateral load to the track through a single center axle. Low speed passes were made with vertical load held constant throughout the testing and lateral load incrementally increased after each set of three passes. The residual lateral displacement was recorded after each pass. The relationship between displacement and the applied lateral load is given in Figure 3-2 with a line shown through the points indicating the displacement after the third pass at each load level. The incremental change in displacement due to each vehicle pass was then calculated. These data

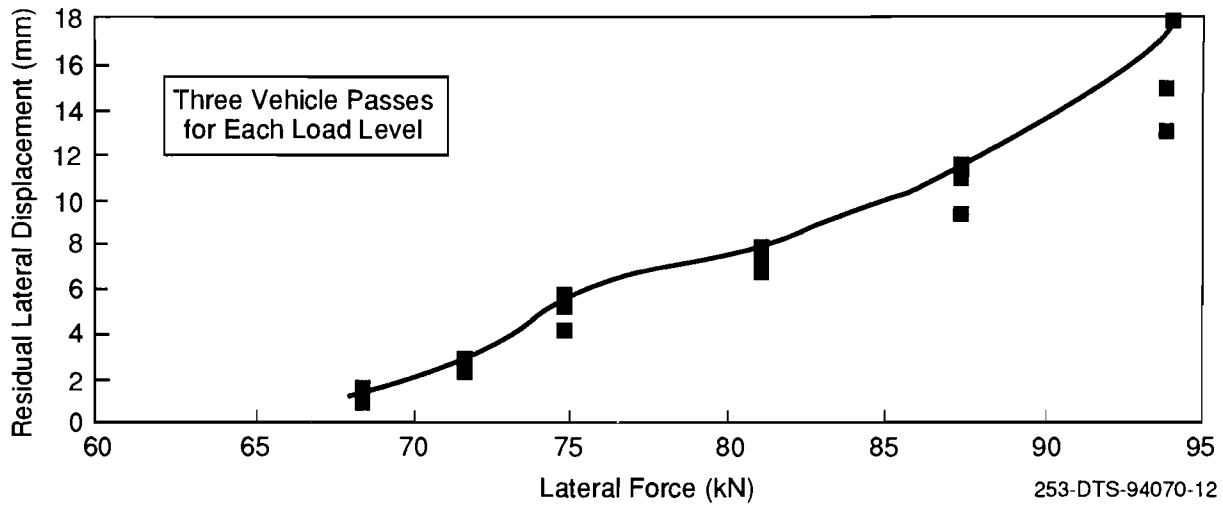

Figure 3-2. The TGV track test data (5)

have been recast to more clearly show the key trend. Figure 3-3 presents the change in displacement for each vehicle pass with the applied lateral load for each group of passes shown across the top of the graph. It can be seen from this figure that the change in displacement decreases for successive passes at a constant lateral load level for all but the last (93.8 kN) level. According to the SNCF, this indicates that the track is stabilizing at these levels and that additional passes would eventually cause no increase in deflection. By contrast, the change in displacement is increasing at the last lateral load level (93.8 kN) and additional passes could be expected to further displace the track to the point of failure. At this load level the track can be considered to be unstable. Therefore, the critical lateral load can be deduced by interpolation between the 87.4 kN and 93.8 kN data points.

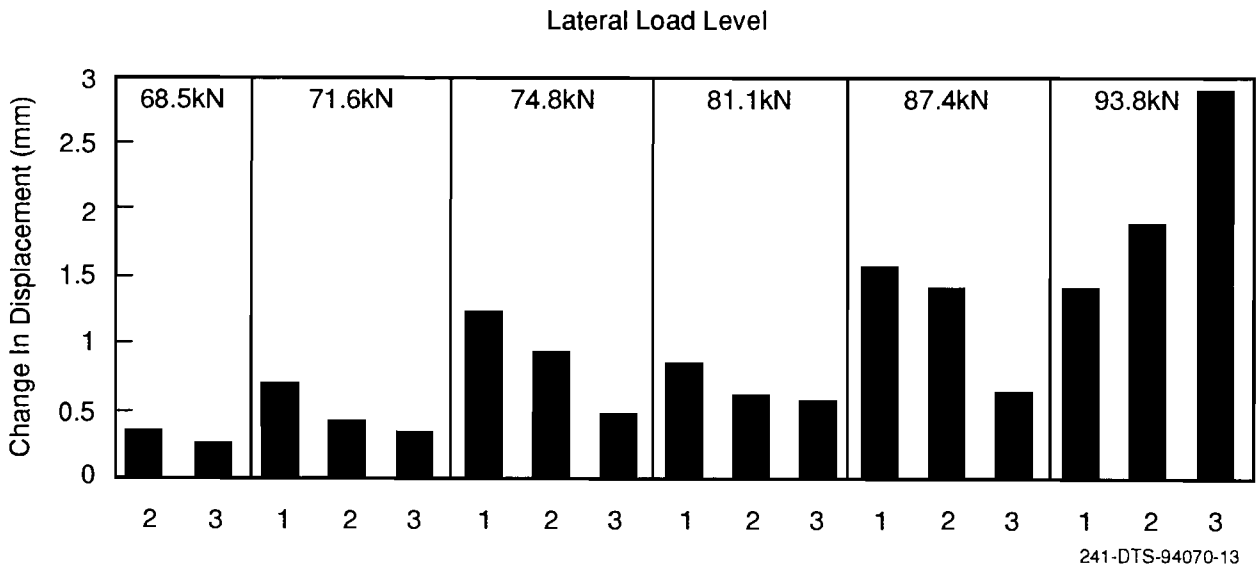

Figure 3-3. Increment in residual deflection (SNCF data, (5))

The SNCF researchers calculated the rate of change of displacement between constant lateral load points. Prior to the highest load level, the rate of change of deflection was negative, indicating a stable condition. At the highest load level, the rate of change was positive, indicating an unstable condition.

These tests were particularly significant in that they present a specific basis for determining the limiting lateral resistance. It would be useful to extend this procedure to address the following considerations:

- The tests were low speed simulations of high speed operations, should, if possible, be conducted at operational speeds to simulate the actual dynamic loads experienced at the wheel-rail interaction.

- The rail thermal loads should also be simulated in the tests to assess their influence on track shift.

ORE Tests

Recognizing the expense and difficulties in conducting the moving load tests discussed above, the primary purpose of the program discussed in reference (6) is to develop an empirical relationship between the limiting lateral load determined through moving load tests and that determined through static load tests on the panel. The tests presented in this report were conducted by Rumanian State Railways (CFR) at Bucharest and were designed to be comparable with previous tests conducted on the same track which are referred to as the "reference track" tests.

Two static test devices were employed during the program. The first applied vertical and lateral loads on a single axle which was apparently pulled laterally by a second vehicle on a parallel track similar to the SNCF "tombereau" vehicle. The second device was a converted tamping/aligning machine which could apply vertical and lateral loads to both rails at the same points (actually 1/2 loads at each of two points approximately 0.5m apart on both rails). Low speed dynamic (moving load) tests were also conducted for comparison. The dynamic tests appear to also have been conducted using the "tombereau" type arrangement.

All tests were conducted on UIC 60 (60 kg/m) rail with wood ties under tamped and 0.04 MGT conditions. Static tests were conducted under both levels of consolidation while dynamic tests were conducted only under 0.04 MGT conditions with vertical loads of 100 and 200 kN. The comparison data for tamped conditions were taken from an earlier ORE report. For each of the two static test consolidation levels, a matrix of seven separate loading scenarios with vertical loads of 67.5, 100, 150, and 200 kN was executed to evaluate the effect of the two loading devices and various loading rates. Negligible difference was observed in the results between the two static loading devices. Significant differences were recorded due to the load application rates.

The data from these tests were analyzed using eight different criteria for determining the limiting lateral load. A linear relationship between the static and dynamic loads was calculated for all load application rates and devices. A criterion was determined to show the best linear relationship for the majority of cases. This criterion defines the limiting lateral load as the load required to deflect the rail by an amount in millimeters equal to one hundredth of the applied vertical load in kilonewtons. For example, if the applied vertical load during a test was 100 kN, then the critical deflection would be (100 x 0.01) = 1 mm. Thus, the critical lateral load would be that which resulted in a deflection of 1 mm.

Recent SNCF Tie Response Tests

Recently tests were conducted by the SNCF (7) to measure the basic response of the individual ties. These tests were conducted to measure the lateral resistance at consolidation levels of 0.015 and 0.10 MGT. The tests were conducted at the Vaires shunting yard between April and June 1991. Seven different tie types were evaluated in sets of two by replacing the rail with two braced, 1.2m long sections of U36 rail. Each set of ties was then loaded laterally up to a deflection of at least 4 mm. The reduced data provide the maximum, minimum, and average lateral resistance per tie at deflections of 2.5 mm and 4 mm for each tie type and consolidation level tested. The oak ties showed an average value of about 3.15 kN/tie at 4 mm after tamping and packing, whereas the corresponding value for the monobloc concrete tie is 11.15 kN. No vertical load was applied on these ties.

While these tests are notable in that they consider the basic tie response characteristics, it would be desirable to extend the work to include the following:

- Vertical load on ties to determine the tie-ballast friction coefficient for use in the analytical methodology.

- Full nonlinear characteristic of tie resistance for deflections larger than 4 mm. Although the maintenance of TGV track limits the deflection to about 4 mm, a much larger critical deflection, δ_c, is of interest in the evaluation of margin of safety, and the ties may exhibit a softening characteristic beyond 4 mm.

Swedish Tests

A test program similar to that reported by ORE (6) was conducted in Sweden (8) to investigate the relationship between S_d and the limiting track strength as determined from a static pull test (S_s). The actual testing involved static loading tests which were then compared to the basic Prud'homme equation. Eight different track configurations were evaluated under three different vertical loading levels (40, 70, and 100 kN). All test sections were tangent track.

The testing vehicle utilized was a converted mail car with hydraulic cylinders mounted at its midpoint. This design was similar to the ORE static test vehicle; however, it introduced load at one point on each rail as opposed to the two point loading of ORE. The vehicle could apply maximum loads of 250 kN (56 kips) vertically and 100 kN (23 kips) laterally. With the vertical load held constant, lateral loading was applied at a rate of 5 kN/sec. The residual deflection was measured after unloading using a tie mounted inductive sensor referenced to a stationary support in the ballast. The limiting lateral resistance was determined using the criterion which was discussed previously.

Linear relationships between the limiting resistance recorded and the Prud'homme equation were fitted to the test data for each track condition. Utilizing the data, S_{stat} values were related to the Prud'homme equation and to the results of the ORE report (6). While linear relationships were evident for each of the static test conditions, the substantial influence of test specific parameters, such as loading rate, appear to limit the applicability of the results of these simpler tests.

Recent tests have been conducted in the United States to qualify the X2000 for operation over the Northeast corridor (9). These tests, which utilized an alternative criterion for track lateral shift (10), are discussed later in subsection 3.5.

3.1.3 SNCF Practice

The SNCF practice of tolerances and load limits for high speed trains may be inferred from the SNCF design and maintenance report (11) and a recent SNCF paper presented at the TRB (12). While the Prud'homme criterion discussed above was developed as a limit for a particular reference track, it has served as a requirement for vehicle performance. During operation of the TGV, deflection limits are utilized to dictate track maintenance operations and adapted versions of the Prud'homme criterion govern vehicle loads. The following operational limits are cited for TGV dual block concrete tie track.

- The maximum repeated lateral axle load which can be applied to the track by the vehicle is defined by 85 percent of the Prud'homme limit; 0.85(10 + 0.33V), with the 0.85 factor used to empirically account for curvature and thermal loads.

- The dual block concrete tie track must be designed such that the static lateral panel resistance equals 24 + 0.41V for tamped track and 38 + 0.63V for stabilized track, with the latter required for summer operations (11). For TGV axle V = 170 kN, this limit equals 93.7 kN for tamped track, and 145 kN for consolidated track. Note that the limiting resistance, here, represents the maximum stationary lateral load that can be sustained by the track under the vehicle vertical loads, without resulting in any permanent displacement of the track panel.

- The rail is manufactured to an initial straightness which typically permits maximum defect amplitudes of 0.5 mm over 2m of rail length. The track construction or realignment tolerance is very low, probably in the range of 1 mm to 2 mm.

- The peak to peak limits for track lateral defects are about 8 mm, below which maintenance may not be required, and 12 mm, above which substantial track repair work will be required, and routine maintenance is not adequate (11).

3.2 British Rail Studies

3.2.1 BR Analysis

Programs to evaluate lateral shift have been conducted by the British Rail along the lines of the SNCF/ORE work. A review of the existing experimental data on track lateral strength and the development of the theoretical analysis of track shift was written by Frederick (4).

A track lateral response model was proposed by Frederick, along the lines of Bijl (13). Attempts were made to quantify the loaded tie resistance. It was concluded that the track segment directly under the wheel loads was generally stable due to the increased lateral resistance, however the resulting track shift due to the vehicle passage must still be limited to avoid buckling of the track portion between the trucks, or after the vehicle passage (static buckling due to thermal loads alone). For the BR track conditions, Frederick derived an expression for the allowable track shift before track buckling is triggered. This is about 6 mm for wood tie curved tracks (R=500m) and 9 mm for concrete tie curved tracks. These limits depend on the track lateral resistance, which is not specified in Reference (4).

3.2.2 BR Tests

After a critical review of the work of SNCF (2), BR conducted tests (4) with particular attention to the effect of ballast consolidation and the influence of larger numbers of vehicle passes. Basic tie response was characterized through single tie push tests (STPTs) of loaded ties to develop relationships between applied vertical load and tie lateral resistance. Moving load tests were then conducted using a loading vehicle design similar to the parallel track

"tombereau" employed previously by SNCF. Typical results of these moving load tests, which were conducted with constant vertical and lateral loads and a large number of vehicle passes, are shown in Figure 3-4. This figure shows the cumulative residual displacement as a function of the number of passes for three different ballast consolidation conditions. The wide range of results for track conditions which were considered similar is to be noted. This range of variation is likely due to the broad qualitative classification of the track conditions and can be reduced if the ballast resistance is quantified and used as a measure of track strength.

Observations based on this work include:

- BR researchers consider it to be difficult to determine the critical vehicle loads on the basis of very small deflections, as derived previously by the SNCF, Figure 3-1.
- A wide "range" was also found in the lateral response of tracks classified simplistically as tamped and consolidated. A more fundamental approach based on the true ballast resistance is required to correlate the critical conditions for the track.

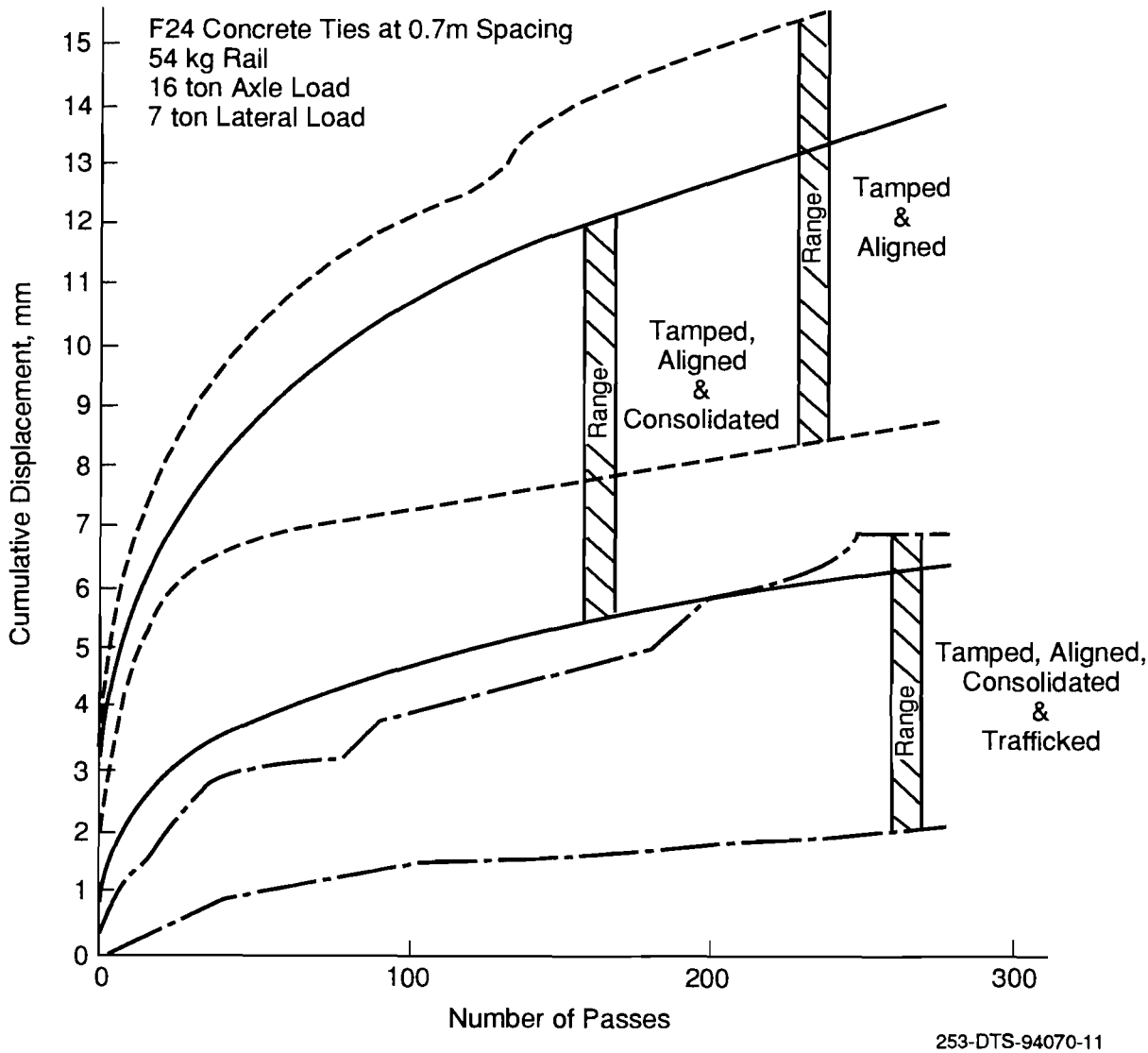

Figure 3-4. British rail track shift test data (5)

3.2.3 BR Practice

British Rail utilizes the Prud'homme limit as a general guideline for vehicle qualification (14). The track is maintained to deflection limits which are apparently based on operational experience.

3.3 Japan (JR) Studies

A general theory for the analysis of track lateral shift is not evident within the available literature. However, a finite element program, DIASTARS, has been developed by JNR for the dynamic response analysis of the Shinkansen cars, on tracks with misalignments (15). Results generated by this program have demonstrated good agreement with experimental results under extreme conditions. While it is not clear if the Prud'homme limit or other lateral force criteria have been used in track and vehicle design, the literature discusses the *permissible lateral deflections and the development of analyses to relate these deflections to safety and ride comfort.* The operational practices of the high speed Japanese Shinkansen lines with respect to track lateral shift are based on deflection limits. An automated mechanized track lining system, AMTLS, which can maintain the track to tight tolerances to minimize lateral forces and accelerations has also been developed (16).

Experiments were conducted with misalignments of up to 30 mm over a 40m chord on the Joetsu Shinkansen line prior to its opening. Test results showed good agreement with the DIASTARS model.

The following operational limits for track lateral shift have been defined. All alignment specifications are made over a 40m chord although future vibration analyses may permit maintenance at various wavelengths. Lateral vibration limits dictate a misalignment limit of 10 mm. *JR companies have set up to 7 mm as the maintenance target.* Tracks are inspected every ten days for distortions. Irregularities can now be controlled to almost within the range of ±2 mm as shown in Figure 3-5, which presents the measured lateral deviation before and after maintenance as a function of the position along the track.

Track geometry management is a broad scoped issue involving numerous considerations of which track shift is only one. While the available literature provides substantial discussions of track geometry, it is unclear what criteria are utilized to limit lateral loads.

3.4 German (DB) Studies

Substantial data have been collected from operations, most notably of the ICE, and these data have been compared with analyses from other sources. Apparently no theoretical

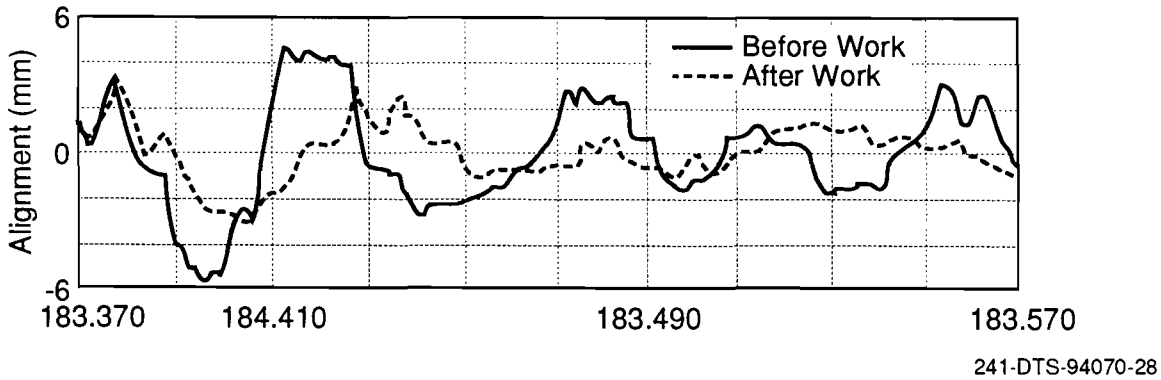

Figure 3-5. JR alignment due to maintenance operations (16)

analyses of track lateral shift have been formulated by DB. The DB indicate that their limits on track lateral shift are based on the related safety issues of derailment and ride comfort although the data used as the basis for formulation of these limits are not clear.

Based on the available literature, the specific use of Prud'homme or other track shift limits is unclear due to the following considerations:

- The Prud'homme limit, is considered to be "outdated" by some researchers (17) while others consider it to be the limit of safe operations (18).
- The Prud'homme limit is "applied only as a target value for vehicle approval" (17).
- Guidelines are not prescribed for limiting lateral deflections in service. In fact the assumption appears to be that no lateral deflection will occur at any time, if the track has sufficient lateral strength.
- The number of vehicle passes are not related to a lateral deflection in order to define maintenance requirements and safety margins.

Recently, vehicle qualification testing of the ICE has been conducted in the United States (19). This program is discussed in the following subsection.

3.5 United States Studies

3.5.1 Track Panel Response Models

Few studies of track lateral shift have been conducted in the United States. However, several basic tools are available for a comprehensive theoretical study of the subject. For example, mathematical models are available for the prediction of track panel shift under vehicle loads, starting from the basic track resistance parameters. These can be extended to repeated loads to determine cumulative residual deflections. Advanced vehicle dynamic models are available to evaluate track lateral loads, e.g., SYSSIM code presented in Section 4.

The response of the track structure to static lateral loads has been characterized in previous work. Tests were conducted at the Transportation Test Center (TTC) in Colorado to measure the response of track panels and individual ties (20). This work developed and validated an analytical procedure for characterizing panel response based on individual tie resistance. However, vertical loading was not applied to the track during these tests. A rigorous track buckling model has also been developed and can be utilized for determining the limiting track shift deflections from a buckling safety point of view. An extensive parametric study (21) was conducted with this model to fully assess the relative influence of various track parameters on the buckling potential.

3.5.2 AAR Laboratory Studies

Laboratory tests investigating loaded track lateral response were conducted at AAR/ Chicago in 1980 and were discussed by Kish (3). The relationships between lateral axle load and track deflection were developed for several different vertical load levels as shown in Figure 3-6. From these data, the relationships between the limiting static lateral track panel resistance and the applied vertical load can be developed and one can possibly correlate the limiting track panel strength as shown in the ORE work discussed earlier.

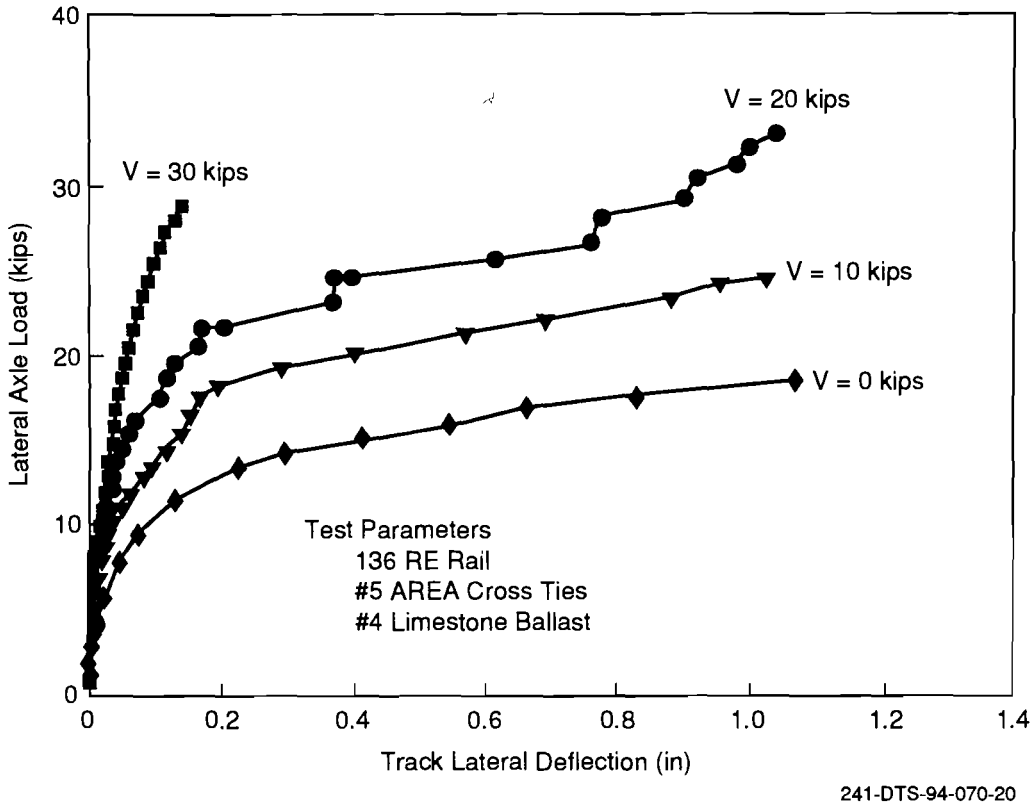

Figure 3-6. Lateral load versus track lateral deflection based on the AAR tests (3)

3.5.3 Vehicle Qualification Tests

Review studies have been conducted by the FRA to evaluate some European designed high speed rail vehicles. For the ICE train, initially considered for the Texas high speed rail system (22), it was stated that the lateral wheel loads should not exceed 85 percent of the Prud'homme limit. For the TGV system (23), the same criterion was cited and data from the TGV tests were reported to be, in general, not more than 57 percent of this limit.

3.5.4 U.S. Tests on the X2000

A test program was recently carried out to qualify the X2000 tilting train for demonstration in the United States (9). Several series of tests were executed including: 1) high cant deficiency tests; 2) high speed stability tests; and 3) demonstration revenue service runs to demonstrate safety in the intended operational environment. The main purpose of the testing was to qualify the vehicles for safety of operation in the planned demonstration tests, and the tests were not intended to develop the track shift criterion.

One of the "stop-test" criteria utilized for these tests was,

$H < 0.5V$

which was apparently based on previous tests (10). This loading limit was never exceeded during the execution of the tests. The Prud'homme limit is not referenced in the test report (9) although the measured loads exceeded this limit as shown in Table 3-1.

Table 3-1. Comparison of vehicle net axle lateral load limits

Criteria	2 deg Curve	4 deg Curve
Prud'homme (10+V/3)	62 kN	62 kN
85% Prud'homme	53 kN	53 kN
0.5V Criterion	78 kN	78 kN
X2000 Test Data	68 kN	66 kN

Although the test report (9) stated that the criterion was not exceeded and that track lateral shift was not observed during the course of the test program, the tests involved a maximum of only 15 passes (approximately 0.006 MGT) through any one curve. Further, more severe conditions such as track imperfections and high compressive thermal load were not simulated. Furthermore, the track lateral strength was not measured. Therefore, although the proposed criterion may be adequate for vehicle acceptance and qualification, further detailed testing on the track is required for use as a track shift criterion.

3.5.5 U.S. Tests on the ICE

A second test program was also recently carried out to qualify the German ICE train for operation in the United States (19). Currently, the available results are limited with only brief discussions of the limiting conditions. As these tests were conducted both to evaluate the ICE and to compare it to the Swedish X2000, it is assumed that the same safety criterion was utilized.

The measured loads did not exceed the limits as per the criterion during testing. However, unlike the X2000 tests, the truckside L/V limit was exceeded in some locations. The condition of the track after testing was not reported. As with the X2000 tests, the number of passes was small. The data may be adequate for vehicle qualification, but additional testing with limiting track conditions is required for an assessment of track shift potential.

3.5.6 Current U.S. Standards

The United States has, to date, no specified limits on vehicle loads and track strength requirements for high speed rail operations. At present the FRA classification (Class 1 to 6) covers speeds up to 110 mph. Clearly, with much higher speeds on modern track likely to be introduced in the United States, the track shift potential increases and the allowable misalignments become much smaller. The tracks will have to be maintained to more stringent specifications for assurance of comfort and operational safety.

3.6 Future Research Needs

The research conducted to date by the SNCF and other researchers has provided a strong basis for the understanding of track shift. Their work has established relationships between the applied vertical load of the vehicle and the lateral strength of the track for particular track structures. Limits for the vehicle applied lateral load have also been established and utilized. These limits, which can sometimes be conservative, have been demonstrated through safe, high speed operation over European tracks with large radius curves. While this work is valuable in support of the development of a rational track shift model for modern U.S. track, significant additional research is required to extend the scope and accuracy of the previous work.

The following future research needs are identified based on this literature review and an assessment of the current U.S. standards for maintenance:

- Establish a relationship between the size of a track defect, its growth or reduction under vehicle passage, and the resultant dynamic component of the lateral load.

- Evaluate the lateral strength of modern U.S. track and determine the allowable vehicle lateral loads from track shift and other safety considerations.

- Develop functional maintenance criteria recommendations for U.S. track which can be used in operation to control the lateral shift.

4. VEHICLE MODEL

In the analysis of track lateral shift, it is necessary to characterize and quantify the lateral loads exerted on the track by vehicle passage. These loads, which may result from curving forces or forces generated during negotiation of a track misalignment, will be used as inputs to the track lateral response models which will be developed in this program. Given these inputs, the track models will then determine the potential for sudden track shift or the growth of track misalignments.

In this section, vehicle dynamic models will be employed for a preliminary investigation of the vehicle lateral forces exerted on the track and the safety limiting conditions arising from track shift. These conditions, which must be investigated to fully determine the overall limiting lateral deflection or load for the track, include:

- Potential for high lateral loads exerted on the track, possibly exceeding the critical track strength.
- Potential for vehicle wheel climb or gage widening derailments.
- Ride quality degradation as the vehicle negotiates the misaligned track.

Ideally, the analysis approach for track shift would include a fully coupled model which accounts for the effects of vehicle-track interaction. Currently, such an interaction model is not available, and existing modeling work has concentrated on development of separate vehicle and track models. In general, this existing work falls into two categories. There exist many complex analyses of vehicles using a simple track model, designed to identify the forces between the wheel and rail up to and including incipient derailment. Other efforts have instead been aimed at modeling the track under a variety of operational conditions and have not included a vehicle model but have used the forces interacting with the rail. This has been the approach derived from the study of track buckling.

An advanced program called SYSSIM, originally developed by Blader, has recently been used to make studies of wheel/rail systems. In this program, the wheel-on-rail rolling contacts are modeled in sufficient detail for the accurate representation of a wheel climb derailment. However, the SYSSIM track model does not include details of the track mechanics behavior. SYSSIM is available for modification to include a continuum rail and track model which would allow valid computation of track response to single and repeated axle passages. As it stands, the SYSSIM model is sufficient to predict the response of any vehicle to track alignment perturbations so long as no deflections of the rail or track accompany the response. The model is used here to give a preliminary assessment of the significance of track shift and its related safety issues.

It is a common engineering practice to express the numerical results obtained in the simulation in the form of certain lateral to vertical force ratios. These ratios are defined in Figure 4-1. These ratios are used in criteria for safety evaluations. For example, the Net Axle Force ratio is used in the track shift empirical criterion (9). The Truck Side Force ratio is applied to predict the gage widening potential. The Single Wheel Force ratio is sometimes used

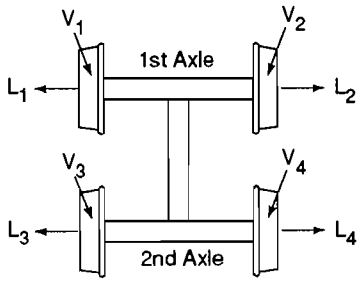

$$\text{Net Axle Force Ratio} = \left(\frac{L_1 - L_2}{V_1 + V_2}\right) \text{ or } \left(\frac{L_3 - L_4}{V_3 + V_4}\right)$$

$$\text{Truckside Force Ratio} = \left(\frac{L_1 + L_3}{V_1 + V_3}\right) \text{ or } \left(\frac{L_2 + L_4}{V_2 + V_2}\right)$$

$$\text{Single Wheel Force Ratio} = \frac{L_1}{V_1}, \frac{L_2}{V_2}, \frac{L_3}{V_3}, \text{ or } \frac{L_4}{V_4}$$

$$\text{Weinstock Force Ratio} = \left|\frac{L_1}{V_1}\right| + \left|\frac{L_2}{V_2}\right| \text{ or } \left|\frac{L_3}{V_3}\right| + \left|\frac{L_4}{V_4}\right|$$

253-DTS-94070-13

Figure 4-1. Lateral-to-vertical force ratio definitions

for wheel climb potential evaluation. A discussion on the state-of-the-art criteria is given in Blader's work (24). The criteria used here are only for the purpose of numerical illustrations and should not be considered as the final tools in the assessments. It should also be remarked that the selected numerical values for the force ratios are the maxima or worst case values from the simulation after the time dependent data have been filtered at 15 Hz, as explained later in this section.

4.1 Preliminary Simulation of a TGV-Type Vehicle

The objective of this work is to formulate a strategy for further investigation of the safety limiting conditions arising from track shift. As an example, the system investigated here is that of a short TGV-type consist with a power car, lead coach and a single articulated car (see Figure 4-2). The suspension characteristics used in this analysis are representative of a high speed vehicle such as the TGV. The track is considered to have an initial sinusoidal lateral misalignment. The peak-to-peak amplitude and wavelength of the sinusoidal misalignment

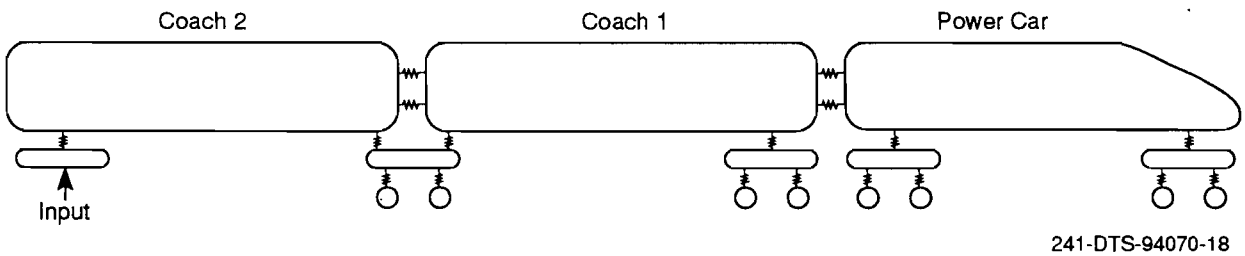

Figure 4-2. Schematic of TGV-type consist model

have been varied in this study to investigate their effects on the lateral to vertical force ratios. Speeds of up to 300 km/hr are considered.

Using the SYSSIM model of the TGV-type consist with the track misalignment, several indicators of unacceptable behavior have been investigated. These include the magnitude of the lateral forces and lateral to vertical force ratios applied to the track, the potential for wheel climb or gage widening derailment, and the deterioration of ride quality.

The use of the computer model in assessing each of these behaviors is described below.

4.1.1 Axle Forces and Net Axle Force Ratios

Primary objectives in the overall analysis of the vehicle-track response are to characterize and quantify the lateral loads exerted on the track, and determine if these loads are sufficient to induce track lateral shift. In the initial analysis performed here, the net axle loads on the track during negotiation of the initial misalignment were calculated using the SYSSIM simulation. These loads were then compared to the 85 percent empirical Prud'homme limit and the overall net effect of the dynamic axle loads on the track misalignment were investigated.

Typical results of the vehicle dynamic response as it negotiates the track misalignment are illustrated in Figure 4-3, which shows the path of one of the vehicle axles through the misalignment. (Note that all results presented here have been filtered at 15 Hz to eliminate any high frequency content in the response, which is not important for this study.) The case shown in this figure corresponds to a vehicle speed of 300 km/hr, with a 12 mm misalignment amplitude and 10m misalignment wavelength. The axle shown is the first axle of the first coach in the consist (in the simulation, this axle typically produced large axle forces on the track). Prior to the misalignment, this axle is centered on the track, with each wheel flange having approximately 10 mm of clearance with the rails, as shown on the figure. As the axle enters the misalignment, the right wheel flange hits the right rail, forcing the axle to the left. After this initial impact, the left flange then hits the left rail at the exit of the misalignment.

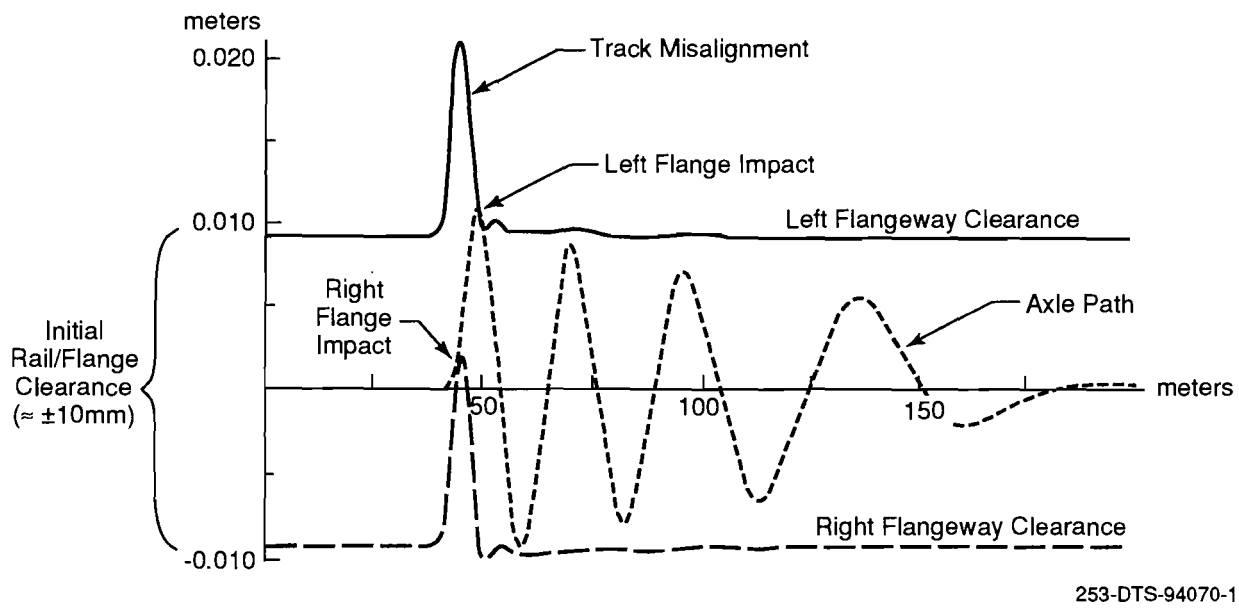

Figure 4-3. Path of axle in flangeway clearance

The axle path then continues to oscillate in the lateral direction before the motion is damped out approximately 100m after the misalignment.

Net Axle Forces

The net axle forces exerted on the track for the case describe above are shown in Figure 4-4, using a vehicle speed of 300 km/hr. As the leading axle (in this case, the first axle of the first coach) enters the misalignment, the right wheel flange hits the right rail, as noted above. This initial impact force of 25 kN (5.6 kips) opposes the direction of the misalignment, as shown on the figure. After the initial impact, a much larger second impact of 55 kN (12.4 kips) occurs when the left wheel flange hits the left rail. This second impact is in the same direction as the misalignment. On a qualitative basis these results indicate that the forces exerted at the entrance of the misalignment would tend to straighten the track, while the forces exerted near the exit of the misalignment would tend to increase its amplitude and/or wavelength. The results also indicate that the axle continues to apply oscillating lateral forces to the track after exiting the misalignment.

Similar lateral force results are presented in Figure 4-5, which shows the net axle force exerted on the track for a vehicle speed of 150 km/hr. The results again show that the initial impact force at the entrance of the misalignment (13 kN, 2.9 kips) would tend to reduce the size of the misalignment, whereas the much larger second impact force (28 kN, 6.3 kips) would tend to increase it. *Thus, for both the 300 km/hr and 150 km/hr cases, the force tending to increase the size of the misalignment is approximately twice the magnitude of the force tending to decrease the misalignment.*

The foregoing numerical examples illustrate that the dynamic lateral force in the misalignment can be significant. Due to the limitation of the track model in the current SYSSIM model, the track response cannot be evaluated. There is also no dependable test data in the literature that can explain the net influence of the dynamic load on the size and shape of the imperfection.

In the absence of a rigorous track response model for moving loads, one approach suggested is to average out the net force in the imperfection and use it as an empirical adjustment to the allowable net axle lateral load. Such an approach is questionable in view of

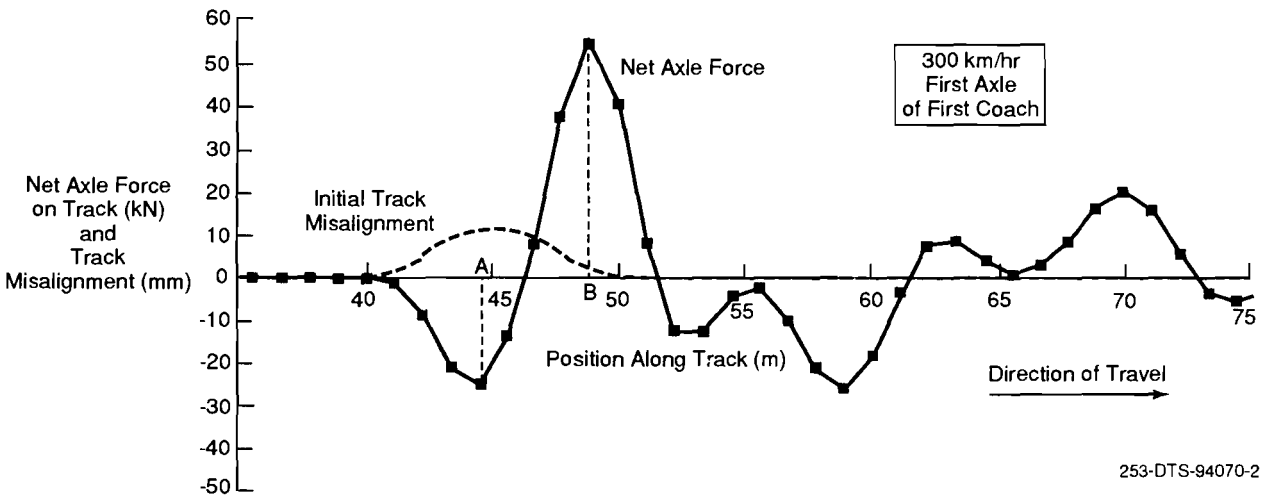

Figure 4-4. Net lateral force on track at 300 km/hr

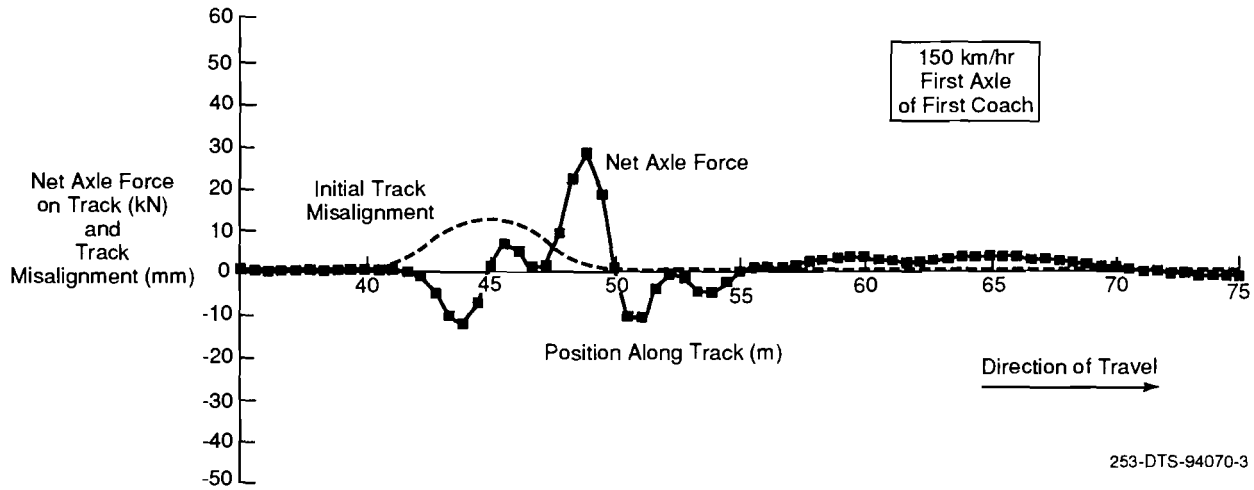

Figure 4-5. Net lateral force on track at 150 km/hr

the relatively small length over which the lateral load is distributed. Static analysis performed in Section 5 of this report showed that generally the lateral load distribution length is 3 to 5m, which is less than the wavelength of the imperfection. Hence, consideration of the peak dynamic force values in the assessment of track shift potential may be justified if they occur at some distance away from one another along the track. Thus, referring to Figure 4-4, the second peak force of 55 kN occurring at point B may contribute to the track shift independently of the first peak at point A. This second peak indeed exceeds the 85 percent Prud'homme limit (46 kN) for this example. Further detailed analysis is required to understand the significance of dynamic components. Clearly, the situation of a curve with an initial imperfection and cant deficiency under a high speed vehicle will show larger track shifting forces due to the combination of steady state curving and dynamic loads.

The simulation has also been used to calculate the net axle force ratio exerted on the track during negotiation of the track misalignment. Sample results for the calculated force ratio are shown in Figure 4-6 for the case of a 12 mm amplitude, 10m wavelength misalignment with a vehicle speed of 300 km/hr. Note that on this figure, the force ratio shows both positive and negative algebraic signs, which correspond to the direction of the lateral force exerted on the track. At the initial impact, the maximum force ratio is approximately 0.19 in the negative direction, tending to straighten the misalignment. At the second impact, the maximum force ratio is approximately 0.41 in the positive direction. (Note that these quantities correspond directly to the net axle forces shown in Figure 4-4.)

The effect of vehicle speed on the maximum resulting net axle force ratio is shown in Figure 4-7 for the case of the 12 mm amplitude, 10m wavelength misalignment. This figure shows that the net axle force ratio increases steadily with increasing vehicle speed, reaching 0.41 at 300 km/hr, as described in the case above. In each case shown on the figure, the maximum net axle force ratio corresponds to a net axle lateral force in the positive direction, occurring near the exit of the misalignment.

Figure 4-8 presents similar results of the net axle force ratio as a function of the track initial misalignment amplitude, for a misalignment wavelength of 10m. These results show that the force ratio increases steadily with increasing misalignment amplitude. For each case shown, the maximum net axle force ratio again corresponds to a net axle lateral force in the positive direction, occurring near the exit of the misalignment.

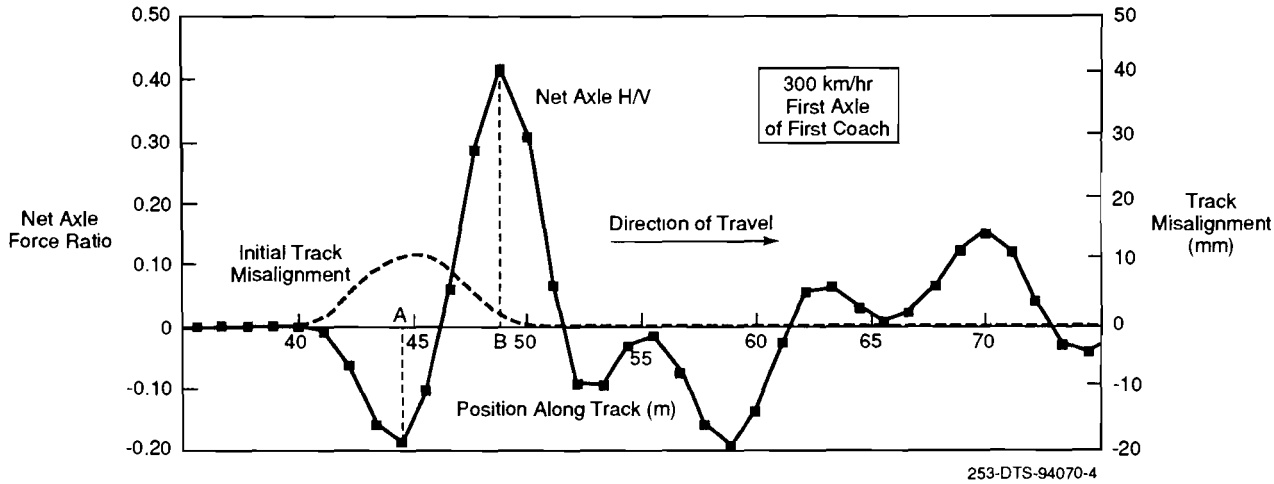

Figure 4-6. Net axle force ratio

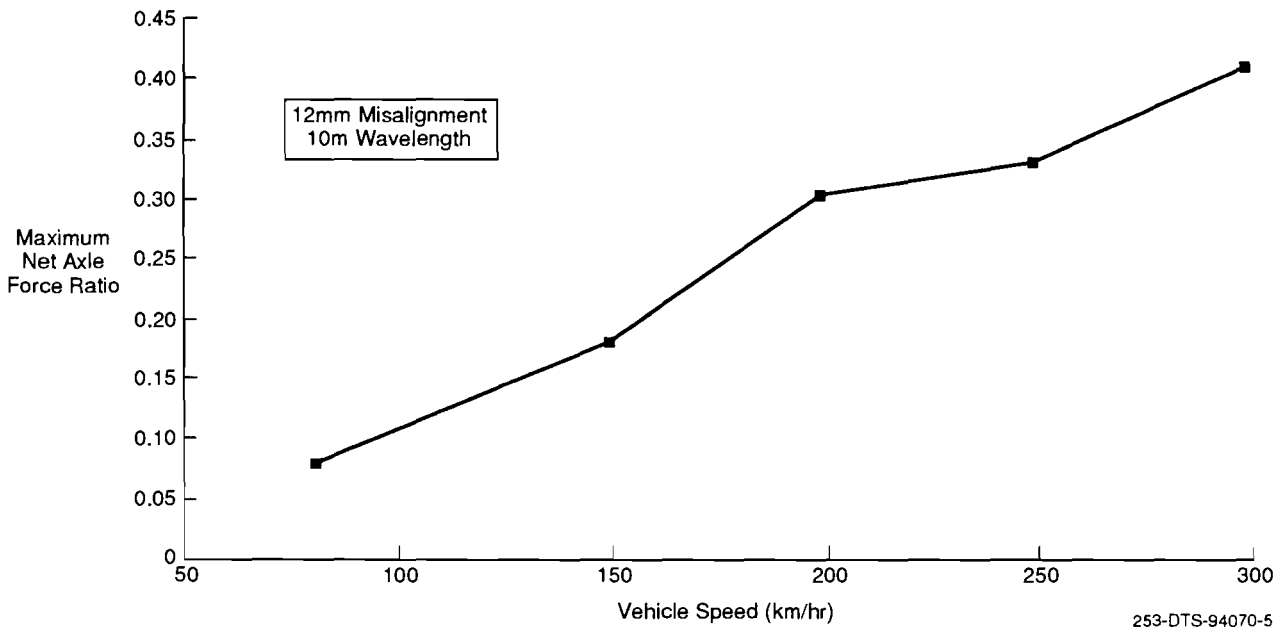

Figure 4-7. Effect of vehicle speed on maximum net axle force ratio

In summary, the results presented here show that the net lateral axle forces and net axle force ratios both increase with increasing vehicle speed and increasing misalignment amplitude. At high speeds (300 km/hr), the lateral forces may exceed desired limits such as the 85 percent Prud'homme limit. The results also indicate that the lateral forces exerted at the entrance of a misalignment tend to straighten the track, whereas the lateral forces exerted at the exit of a misalignment tend to increase the misalignment size. The relative magnitudes of these forces indicate that their combined effect would tend to increase the overall size and/or wavelength of the misalignment.

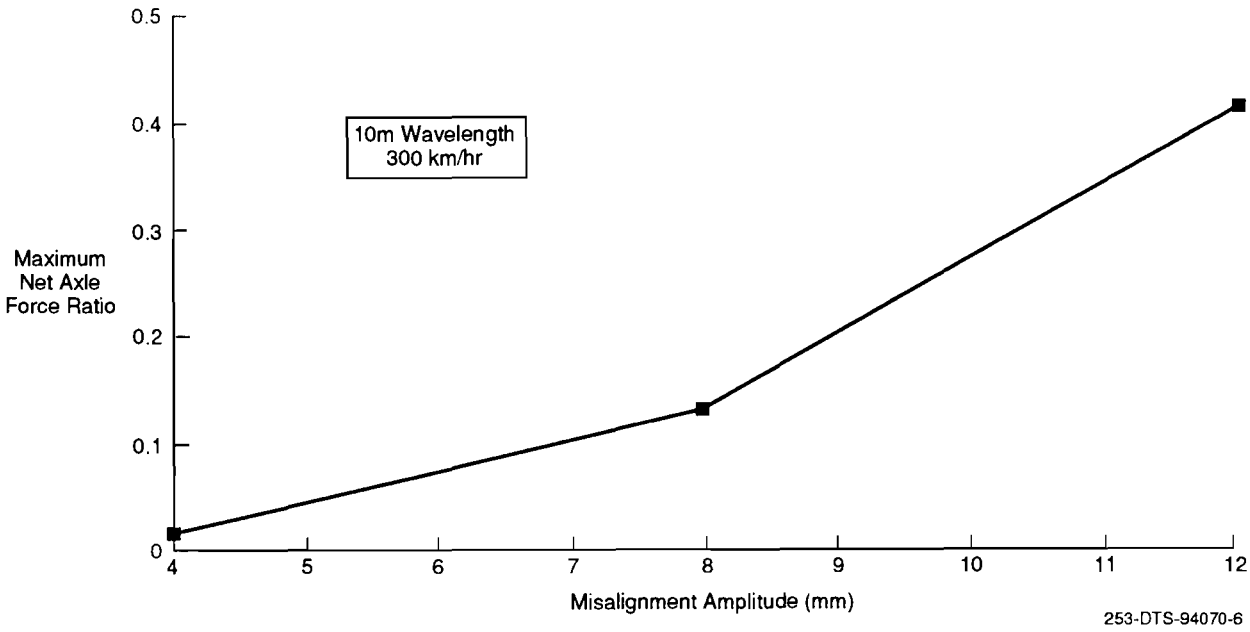

Figure 4-8. Effect of misalignment amplitude on maximum net axle force ratio

In addition to determining the lateral forces and force ratios applied to the track (as shown by the preceding examples) the computer simulation is also useful for investigating other safety limiting conditions arising from track shift. These conditions include the potential for wheel climb derailment, the potential for gage widening derailment, and the degradation of ride quality. The use of SYSSIM in assessing each of these conditions for the TGV-type consist is discussed in the following subsections.

4.1.2 Wheel Climb Derailment

As explained previously, the computation of the rolling contact forces in SYSSIM allows a representation of wheel climb derailment which is not dependent on any lateral-to-vertical wheel force ratios. During a computer run, the model automatically indicates when a wheel climb derailment has occurred, at which point the simulation is ended. The present model of rolling contact is thought to be slightly conservative, i.e., it predicts a derailment slightly more easily than would be seen in the real world for the same case. This is primarily due to an approximation in the third dimension at the contact angle used to speed up the calculation.

The wheel climb derailment results for cases studied in this analysis are summarized in subsection 4.2.

4.1.3 Ride Quality

Serious deterioration of ride quality may also lead to an unsafe condition for the passenger, particularly when standing. Several recent studies have suggested values for the peak-to-peak lateral acceleration which were unacceptable. These values will vary with any unbalanced lateral acceleration. A comprehensive discussion of this issue has been given by Eickhoff [25]. Other values suggested are slightly more conservative [26]. A value of 0.12g peak-to-peak has been used in this study as a threshold to raise concerns on the ride quality issue during passage through the track misalignment.

The peak-to-peak lateral acceleration results for cases studied in this analysis are presented in the following summary.

4.2 Summary of Simulation Results

Tables 4-1 and 4-2 summarize the results of the SYSSIM simulation studies for the TGV-type consist at speeds of 300 and 150 km/hr, respectively. Each table lists the calculated net lateral axle forces, peak-to-peak lateral accelerations, truckside force ratios and the occurrences of wheel climb derailment for several combinations for misalignment amplitude and wavelength. As noted previously, the results shown in these tables have been filtered at 15 Hz to reduce the high frequency content of the response. The results are described below.

The net lateral axle forces generally increase with increasing speed and misalignment amplitude. At high speed (300 km/hr), for several cases of 12 and 20 mm misalignment, the 85 percent Prud'homme limit is exceeded, and this frequently coincides with a wheel climb derailment. For misalignments of 8 mm or less, the net axle forces are less than 30 kN and are well below the 85 percent Prud'homme limit.

The results also indicate that wheel climb derailments are likely at the largest misalignment amplitude of 20 mm peak-to-peak, especially at the 300 km/hr vehicle speed. Ride quality also appears to be marginal at misalignments greater that 12 mm, especially at 300 km/hr. Truckside force ratios are also largest for the large misalignments (12 and 20 mm).

Based on these results, it appears that misalignments of 12 mm or greater mark the onset of higher lateral track forces, degraded ride quality, and increased derailment potential for the

Table 4-1. Summary of SYSSIM results for 300 km/hr

Misalignment (mm)	Wavelength (m)	Max Net Axle Lateral Force (kN)	Jolt Peak-to-Peak Lateral Accel. (g)	Max Truckside Force Ratio	Wheel Climb Derailment
4	8	<2	<0.05	0.02	-
8	8	<30	0.07	0.16	-
12	8	54*	0.11	0.40	-
20	8	-	-	-	Yes
4	10	<2	<0.05	0.02	-
8	10	<30	0.08	0.16	-
12	10	55*	0.12**	0.39	-
20	10	-	-	-	Yes
4	15	<2	<0.05	0.02	-
8	15	<30	0.08	0.18	-
12	15	59*	0.13**	0.40	-
20	15	-	-	-	Yes
4	20	<2	<0.05	0.02	-
8	20	<30	0.08	0.19	-
12	20	53*	0.13**	0.39	-
20	20	82*	0.15**	0.50	-

Notes:
Values not listed for derailed cases.
*Meets or exceeds limit of 0.85 (10 + V/3) for this case.
**Meets or exceeds desired limit of 0.12g peak-to-peak lateral acceleration.

Table 4-2. Summary of SYSSIM results for 150 km/hr

Misalignment (mm)	Wavelength (m)	Max Net Axle Lateral Force (kN)	Jolt Peak-to-Peak Lateral Accel. (g)	Max Truckside Force Ratio	Wheel Climb Derailment
4	8	<2	<0.05	0.02	-
8	8	<30	0.09	0.14	-
12	8	<30	0.07	0.24	-
20	8	-	-	-	Yes
4	10	<2	<0.05	0.02	-
8	10	<30	0.08	0.13	-
12	10	<30	0.08	0.23	-
20	10	-	-	-	Yes
4	15	<2	<0.05	0.02	-
8	15	<30	0.09	0.16	-
12	15	<30	0.10	0.19	-
20	15	43	0.14*	0.32	-
4	20	<2	<0.05	0.02	-
8	20	<30	0.08	0.16	-
12	20	<30	0.10	0.16	-
20	20	<30	0.15*	0.24	-

Notes:
Values not listed for derailed cases.
*Meets or exceeds desired limit of 0.12g peak-to-peak lateral acceleration.

type of vehicle investigated here. For 20 mm misalignments, the potential for wheel climb derailment is very high, with derailment typically preceding any serious degradation of ride quality. Further work is required to examine the limits the misalignment amplitude and the influence of curvature.

4.3 Conclusions of Simulation Studies

1. Use of vehicle dynamic models such as the SYSSIM simulation code will be important in the evaluation of dynamic loads generated by the vehicles as they negotiate track irregularities. The dynamic loads are required for the misalignment growth and track shift studies. The SYSSIM model will also serve as a tool for the assessment of derailment potential due to wheel climb, and ride quality degradation. As such, the model can evaluate the permissible limits of track misalignments, track shift and vehicle speed.

2. The dynamic lateral axle loads applied to the tangent track during negotiation of a track misalignment can generate large track shifting forces (peaks exceeding the 85 percent Prud'homme limit). These loads, and the corresponding net axle force ratios, increase with increasing vehicle speed and misalignment amplitude.

3. When the vehicle enters a sinusoidal misalignment on tangent track, the initial axle impact force opposes the direction of the misalignment, and would tend to straighten the track. However, near the exit of the misalignment, the vehicle also applies a second impact force. This second impact force is typically much larger than the first, and is in the direction of the initial misalignment, which would tend to increase the misalignment amplitude or wavelength. Further work is required to quantify the track response under the dynamic loads generated at the track irregularities.

4. Wheel climb derailments can occur at misalignment amplitudes of 20 mm, even at the lower vehicle speed of 150 km/hr, whereas at higher vehicle speeds (300 km/hr), derailments may occur at misalignments of 12 mm or greater for the type of high speed vehicle studied here. When a derailment occurs, the simulation indicates that it typically precedes any serious degradation of passenger ride quality, meaning that up to the instant of wheel climb derailment, the peak to peak lateral accelerations are not severe. Obviously, serious degradation of ride quality will occur immediately after this point. Ride quality is also degraded for cases which did not derail. However, ride quality may not be the determining factor for all vehicles. For vehicles with body tilting mechanisms negotiating cant deficient curves, wheel climb derailment and track shift potential may be the limiting conditions, although the tilting vehicles and curves are not simulated in the present study.

5. TRACK SHIFT MODELING AND TEST REQUIREMENTS

As stated in Section 3, the only available theoretical work on the track panel shift is that of the SNCF (2). This work calculated the panel response under a single monotonically increasing lateral load and under a constant vertical load. The SNCF work was instrumental in defining the limiting lateral loads for track shift for their specific track design. Advancements in track design and analysis now permit a more rigorous evaluation to fully establish the capacities and limitations of modern track. Computation of track shift can now be performed based on more accurate vehicle loads and an appropriate track structure model. The requirements of this advanced model are:

- It must be capable of predicting the cumulative deflection of the track panel under loading and unloading cycles, and moving loads.
- It must rigorously account for the loaded nonlinear dynamic resistance of the ballast.
- It must include thermal and curvature effects.

5.1 Load Inputs

Development of appropriate load descriptions involves issues such as stationary versus moving loads, quasi-static versus time varying loads, and single axle versus truck versus two truck loads (3). Models will have to be constructed to identify the critical load characteristics required in the track shift quantification. The issue of track dynamics should also be resolved in a future modeling study. The immediate need exists to study the basic problem of the track panel response under loading and unloading cycles and evaluate the cumulative residual deflection as a function of cycles. The following method will be used for the analysis of the problem.

5.2 Track Panel Structural Model

The objectives of this model are:

- To determine the limit load level on the track for sudden panel shift or the onset of significant track shift.
- To determine the cumulative residual deflection due to cyclic loading below the limit load.

The required analysis consists of the following important parts:

- Determination of *vertical load distribution* on ties.
- Evaluation of the resulting *lateral resistance distribution*.
- *Lateral deflection response* evaluation under vehicle and thermal loads, accounting for curvature effects.

- Evaluation of track panel limit load.
- Evaluation of *residual deflection* after unloading.

These are discussed in the following subsections.

5.2.1 Vertical Load Distribution

The lateral track response under lateral loads is significantly influenced by the vertical load distribution on ties due to the sensitivity of tie-ballast frictional forces to the vertical load. Evaluation of the vertical load on ties requires the vertical foundation stiffness parameter. This is a relatively straightforward task, if the vertical track modulus is assumed constant. If the track vertical stiffness is nonlinear, as is usually the case, the solution is involved. An assumption can be made that the track vertical stiffness can be considered linear up to some value of vertical deflection (typically 0.1 in.) and nonlinear beyond that. Figure 5-1 shows this vertical stiffness characteristic. Figure 5-2 shows the track structure model for vertical

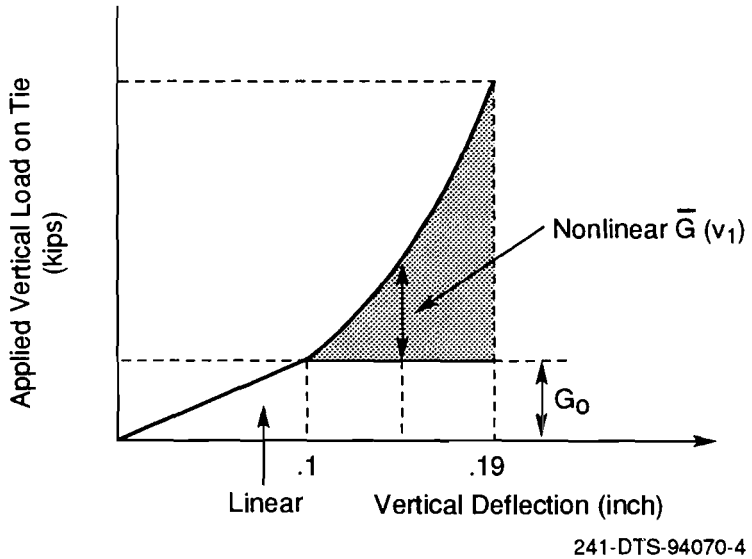

Figure 5-1. Track vertical stiffness idealization

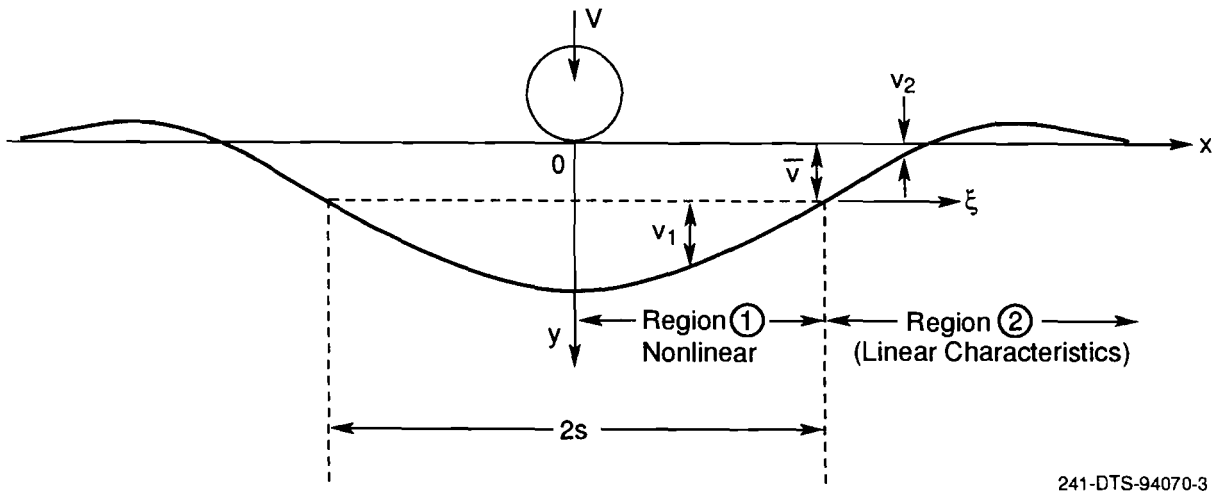

Figure 5-2. Track model for vertical deflection

deflection analyses. The differential equations and a solution technique for the vertical deflection are presented in Appendix A.

Numerical Example (TGV Axle Load)

Numerical results from the formulation presented in Appendix A yielded the relationship between applied load and the track vertical deflection, shown in Figure 5-3a. The track self weight Q is ignored in this analysis, since the given vertical stiffness characteristic is assumed to be with respect to added load on the track. The characteristic is linear up to $\bar{v}$ = 0.1 in., and nonlinear beyond this. Preliminary calculations for the track vertical response are shown in Figure 5-3b.

The TGV axle load (assumed to be at 37.4 kips or 166.4 kN) gives a deflection of 0.093 in. (2.4 mm) and is within the linear regime for the given track characteristic. For an assumed self weight (Q = 3.5 kN/m), there is a additional downward deflection of 0.005 in. (0.13 mm).

Vertical Load Distribution

The vertical load distribution is calculated from

$$R_v = k_v v + Q$$

where

R_v = vertical ballast reaction
k_v = vertical stiffness
v = vertical deflection

Figure 5-4 shows the resulting load distribution on a typical track with ties spaced 24 in. apart. Note that the center tie carries approximately 27 percent of the total vertical load.

5.2.2 Lateral Resistance Distribution

The distribution of the ballast resistance can be calculated from the load distribution on the ties. Depending on the levels of consolidation, the lateral resistance of a single tie without vehicle loads exhibits a characteristic as in Figure 5-5. Extensive data have been collected for wood ties (20) and studies to characterize concrete tie resistance are now being planned by the Volpe Center. Highly consolidated wood tie tracks showed softening (drooping) characteristics beyond a lateral displacement, w_p ($\simeq$ 0.25 in., 6 mm), but the resistance levels off beyond a limiting deflection value, w_L, ($\simeq$ 6 in., 150 mm). Freshly tamped tracks showed a constant resistance beyond a certain displacement (also represented by w_p, for convenience). Hence, the static (with no vehicles) resistance of consolidated track can be represented by the four parameters, the peak resistance (F_p), the deflection at peak resistance (w_p), the limit resistance (F_L), and the deflection at limit resistance (w_L) and that of freshly tamped tracks by w_p and F_p. In view of the relatively smaller deflections (< 2 in., 50 mm) that are of interest in track shift analyses (compared to track buckling), w_L and F_L may not be important parameters for track shift, although the drooping part may still have to be incorporated up to a certain deflection level ($\approx$ 2 in. 50 mm). When the ties are loaded vertically, the initial resistance part tends to be stiffer, and the resulting characteristics are as indicated in Figure 5-5. The value of w_p for the loaded ties may be assumed to be the same as in the static case.

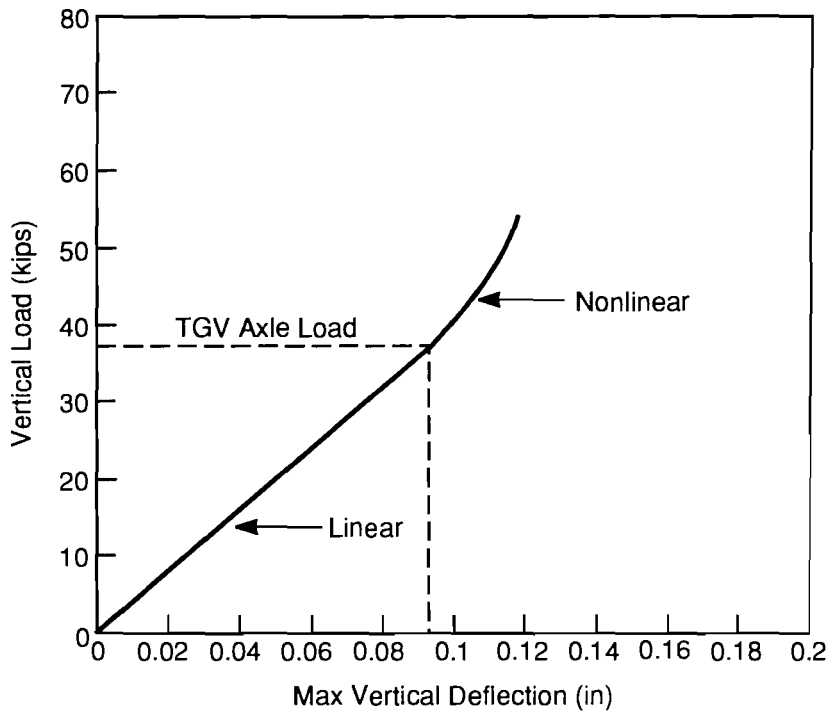

(a) Vertical Response

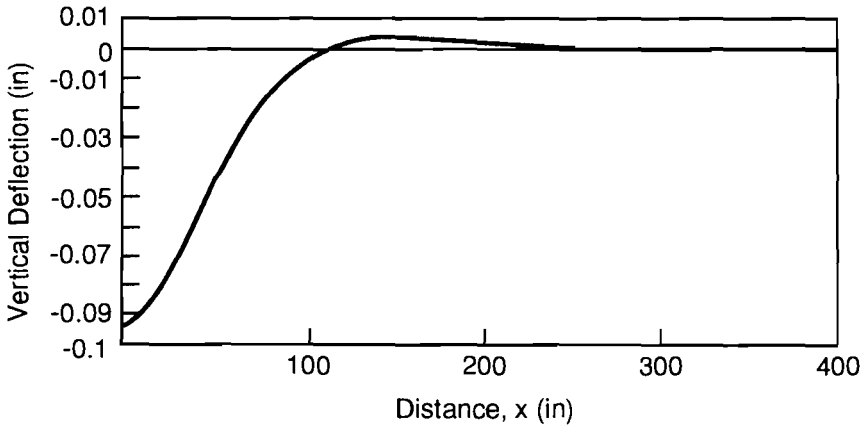

(b) Deflection Profile for TGV Load

204-P-93883-9

Figure 5-3. Numerical result for vertical deflection response

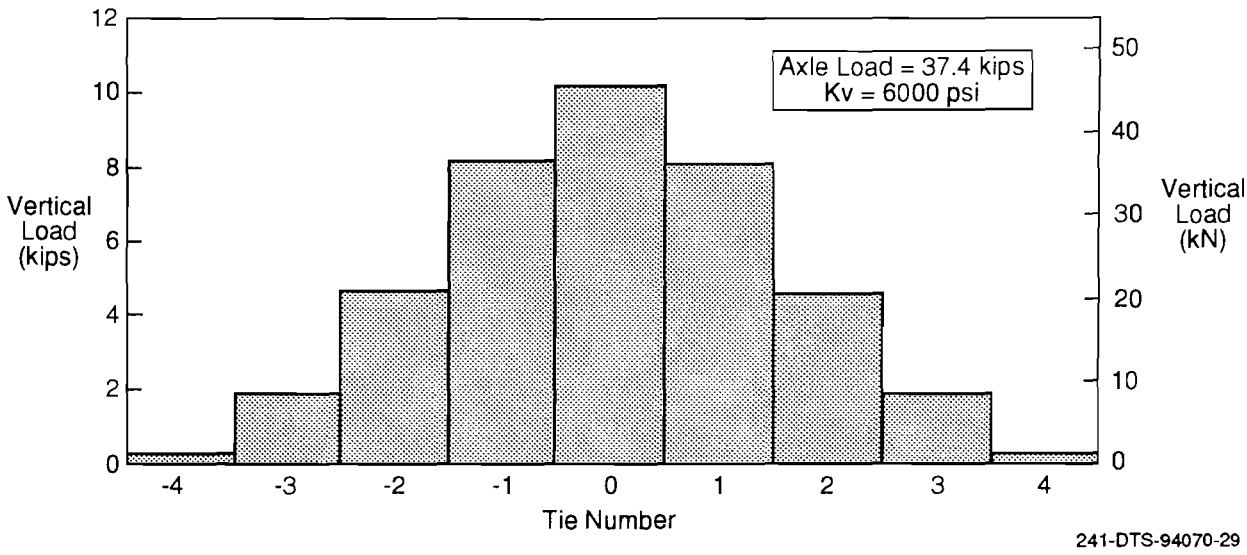

Figure 5-4. Distribution of the vertical tie reaction load

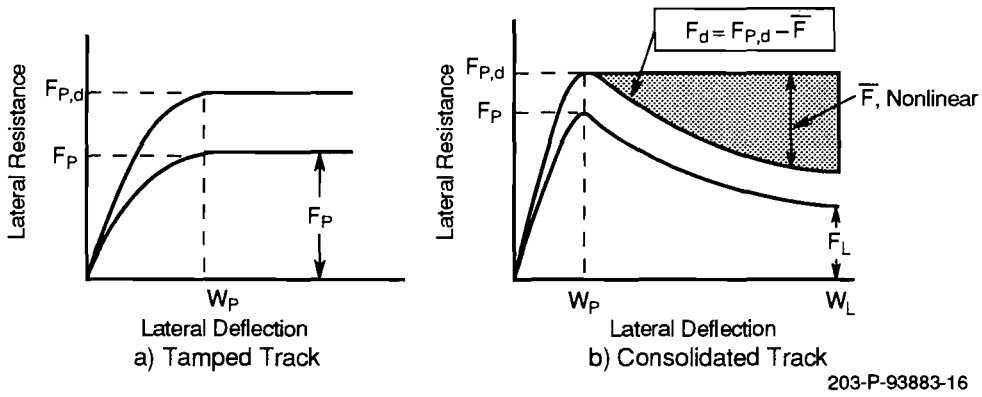

Figure 5-5. Typical lateral resistance characteristics

It has been shown that the tie resistance has three significant components: the base, the side friction, and the end shoulder (20). For loaded ties, the base friction changes. The loaded resistance can be expressed as:

$$F_{base\ (dynamic)} = F_{base\ (static)} + \mu_f R_V \qquad (5\text{-}16)$$

where μ_f is a coefficient and R_v is the vertical load on the tie. The coefficient μ_f is to be determined from tests, and may be a function of R_v, for given tie and ballast conditions. Limited data on μ_f for conventional wood tie track exist, but need to be determined for high speed track with concrete ties. The expected variation of F_{base} with respect to R_v is shown in Figure 5-6, from which μ_f can be evaluated. Note that when R_v equals -Q, where Q is track weight, the base friction falls to zero, which will be the case in the track uplift region, at some distance away from the load point.

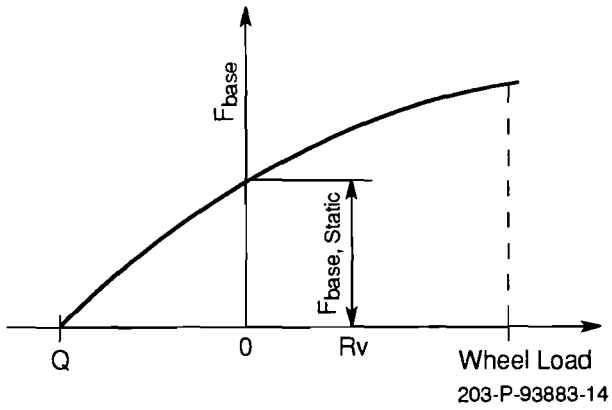

Figure 5-6. Typical variation of base friction

5.2.3 Lateral Response of Track Panel

The track panel lateral response can be determined with the knowledge of the lateral resistance distribution as derived in the previous subsection. The lateral deflection of the track is divided into two regions as indicated in Figure 5-7. The "tie" deflection at limit resistance (w_p) will be considered as the deflection beyond which the track accumulates significant residual deflections.

- Region I represents deflections larger than w_p of the lateral resistance characteristic. The lateral resistance in this region is constant in the case of the tamped track or "drooping" in the consolidated condition. The lateral resistance is also a *function of the distance* from the wheel location.

- Region II represents deflections less than w_p. The lateral resistance is assumed to be proportional to the lateral displacement. The lateral stiffness is a function of the distance coordinate.

The differential equations for the two regions are straightforward. Region I will have linear or nonlinear differential equations (depending on tamped or consolidated track conditions), whereas Region II will have a linear differential equation with a *variable* coefficient. Because Region II is truncated at a finite distance, the boundary conditions will involve the transversality condition of zero moment in addition to the zero deflection and slope conditions at the ends. These boundary conditions and the conditions of continuity (on deflection, slope, moment and shear force) at the common point between the two regions can be satisfied using Fourier series and an iteration technique. Details of the solution are presented in Appendix B.

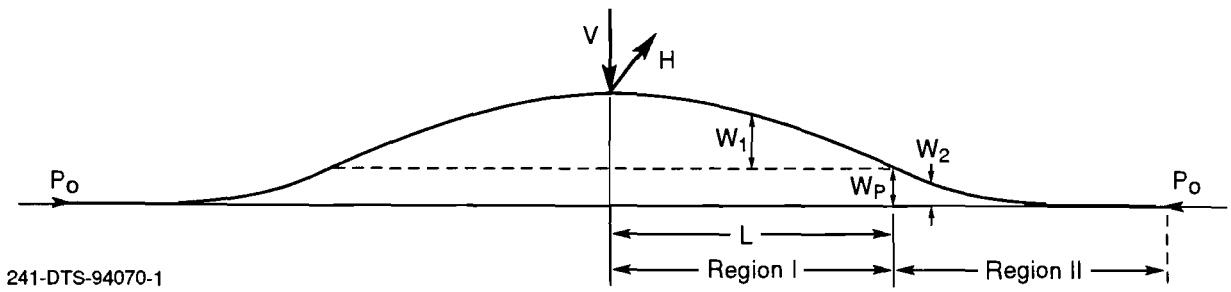

Figure 5-7. Lateral response model

Numerical Results

Numerical results are presented here for the special case when the lateral deflection just reaches the limit defined by w_p. The required lateral load for this deflection will be defined as the track static lateral load limit, S_l. Clearly, for $H > S_l$, the ballast lateral resistance limit will be exceeded for some ties in the central zone, and there will be significant residual deflection after the wheel passage (unloading). It is of practical interest to evaluate S_l as a function of the following parameters, as it represents an upper bound for track strength.

$$S_l = f(V, F_{P,S}, \mu_f, k_V, \Delta T, R)$$

where

V = axle vertical load
$F_{P,S}$ = peak value of ballast lateral static resistance
μ_f = tie-ballast friction coefficient
k_V = track vertical stiffness
ΔT = rail temperature over the neutral
R = track radius

Table 5-1 presents the assumed parameters for the numerical study. The tie limiting deflection, assumed to occur at the peak value of the resistance, is set at w_P = 6.4 mm (≈ 0.25 in.) [21]. The torsional stiffness of the fasteners is neglected for simplicity in the preliminary assessments.

As shown in Appendix B, the solution of the problem is developed using Fourier series. This results in an infinite system for simultaneous equations for the Fourier coefficients. For numerical work, the first five harmonics are considered. The convergence of the series is fast as seen from Figure 5-8 which compares the results from one, two and five harmonics with the exact solution. The lateral stiffness increment represents the quantity ($\mu_f R_v$) divided by w_p. (See Equation 5-16.)

Table 5-1. Assumed track parameters

Parameter	Units	Range	Nominal Value
Axle vertical load	kips	20 to 50	37.4
	kN	89.0 to 222.4	166.4
Static lateral resistance peak, F_P	lb/in.	50 to 200	100
	kN/m	8.8 to 35.0	17.5
Tie-ballast friction coefficient	-	0.4 to 1.0	0.5
Track vertical stiffness	psi	2000 to 10,000	6000
	MPa	13.8 to 69.0	41.4
Rail temperature over neutral	°F	0 to 75	0
	°C	0 to 41.7	0
Track curvature	deg	0 to 8	0 (tangent)

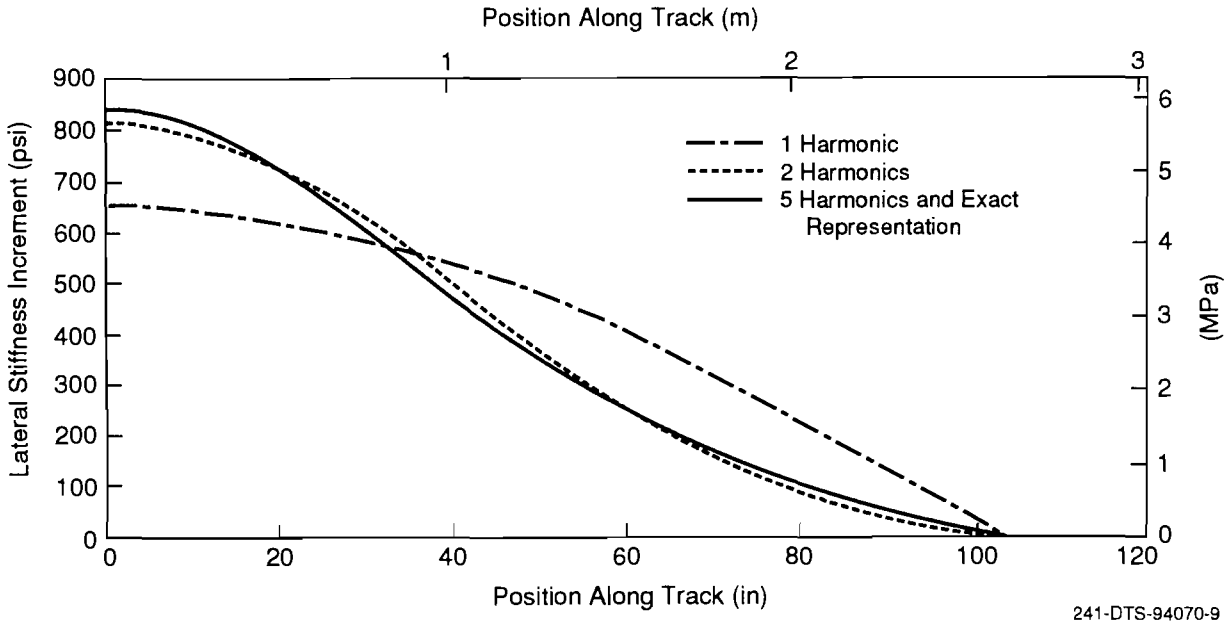

Figure 5-8. Fourier series approximation to lateral stiffness contribution by vertical load (k_v = 6000 psi, V = 37.4 kips)

The following parametric study is performed using the parameters in Table 5-1. The "variable" in the study is over the range specified and other parameters assume the nominal values in the table.

1. *Effects of Axle Vertical Load* - The axle vertical load has a stabilizing effect as seen from Figure 5-9. For an assumed axle load of 37.4 kips (for a TGV type car), the lateral load limit for the track lateral response to be within the tie deflection limit of 0.25 in., is about 22 kips (97.9 kN). A 10 percent increase in the axle load will increase the lateral limit load by about 5 percent.

2. *Effect of Ballast Lateral Resistance* - This is an important parameter governing the lateral strength of the track. As seen in Figure 5-10, for some weak tracks (after lifting and tamping operations), the resistance can be as low as 50 lb/in. which gives a value of about 18 kips (80 kN) for the load limit. For strong tracks ($F_{P,S}$ = 200 lb/in.) this value increases to about 29 kips (129 kN).

3. *Effect of Tie-Ballast Friction Coefficient* - A high tie-ballast friction coefficient is clearly desirable as it increases the track lateral resistance. Figure 5-11 gives the results for S_e over a possible range of field values. The low friction coefficient of 0.4 represents concrete ties with a smooth bottom surface. The higher value of 0.8 is typical for modern concrete tie track with granite ballast.

4. *Effect of Track Vertical Stiffness* - Figure 5-12 shows the results for the lateral limit load, S_l, over a typical range of track vertical stiffness. Over the range (2,000 to 10,000 psi), of the vertical stiffness, the variation is apparently small (<5 percent). This needs to be confirmed by further detailed analysis.

5. *Effect of Temperature and Curvature* - Because the deflections are small, the rail temperature effect on the lateral load is small in the case of the tangent track. However, for the curved track the effect appears to be significant (Figure 5-13 shows the relationship between the limit load S_l, the rail temperature above neutral, and the track curvature for assumed elastic displacement of 0.25 in.). The radial movement (breathing) of the curve

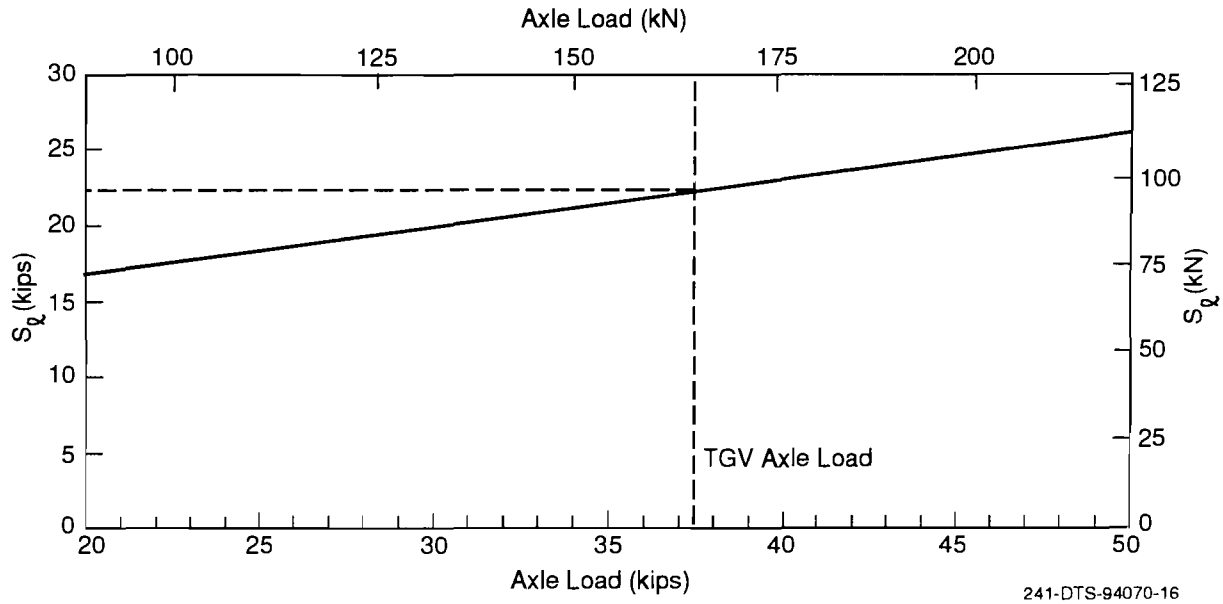

Figure 5-9. Effect of axle vertical load on panel lateral limit load

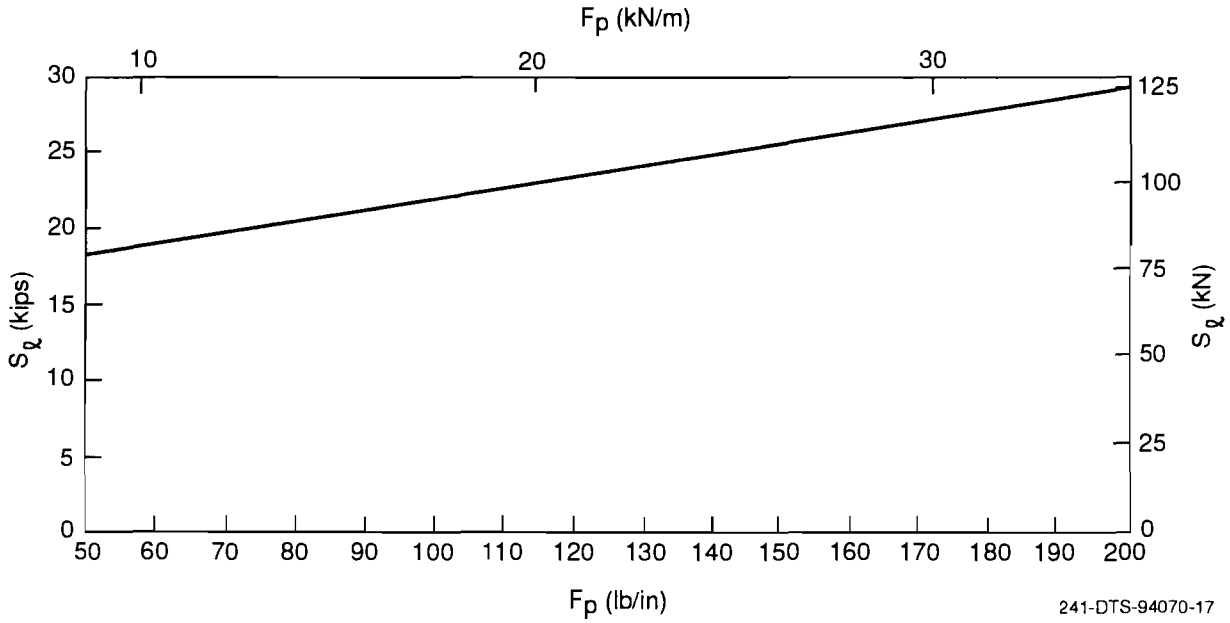

Figure 5-10. Effect of ballast lateral resistance on panel lateral limit load

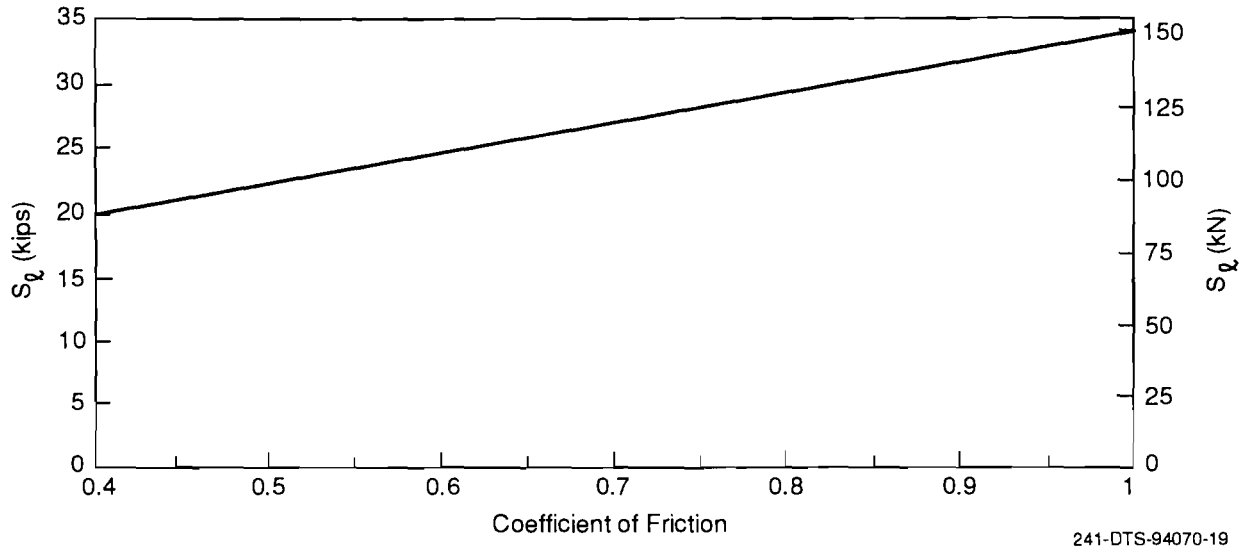

Figure 5-11. Effect of tie-ballast friction coefficient on panel limit load

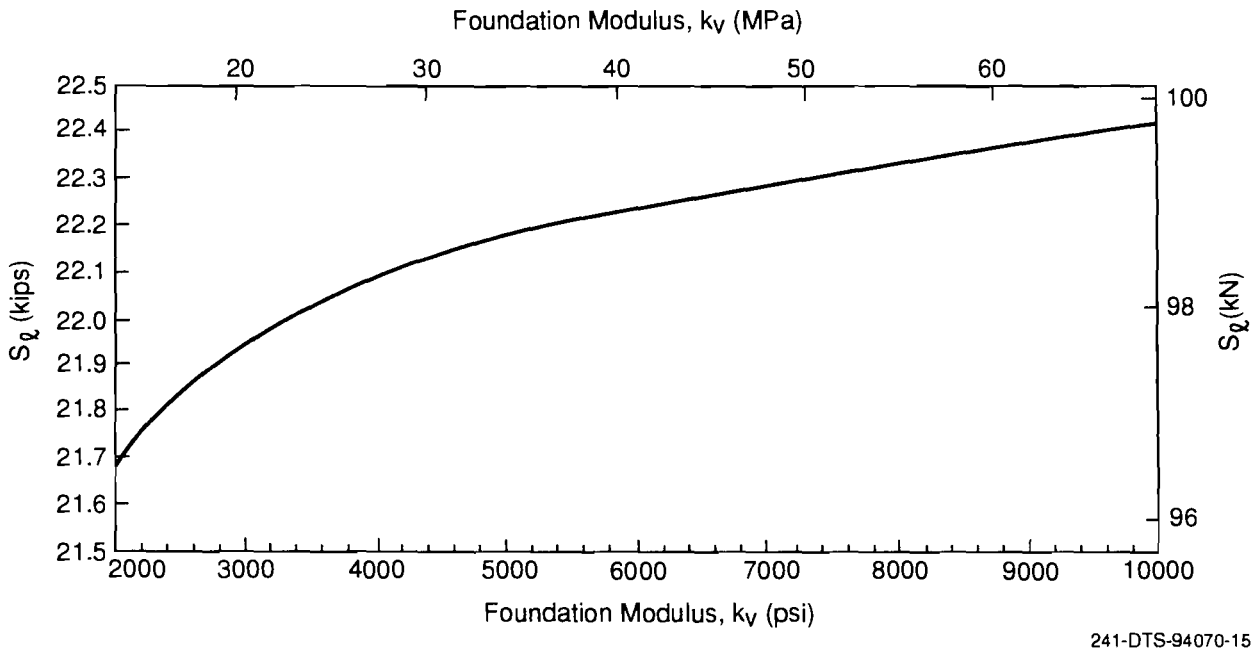

Figure 5-12. Effect of vertical stiffness on panel lateral limit load

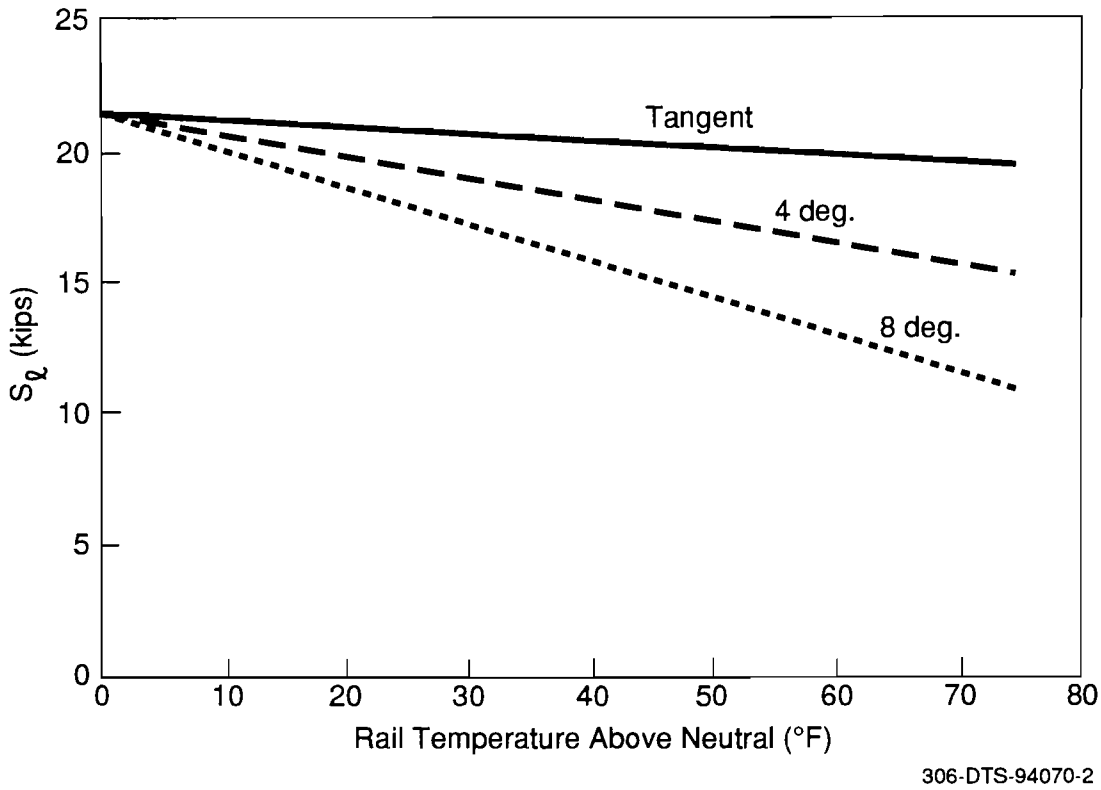

Figure 5-13. Effect of temperature and curvature on panel lateral limit load (w_p= 0.25 in.)

under the influence of temperature reduces the limit in the curved track as compared to the tangent track. For example, the 4 deg curve will move radially outwards under thermal load alone (ΔT=75°F) and to reach a total deflection of 0.25 in., requires a lateral load of 15.2 kips. The 8 deg curve requires a load of 10.8 kips. Of course, such high degree curves are seldom used for high speed passenger transportation. This study may be of practical interest in the freight transportation on slow speed tracks on which large lateral loads can be generated due to relatively large initial misalignments permitted, or due to inadequate superelevation.

5.2.4 Comparison with Existing Empirical Limits

It is of interest to compare the limiting static strength of the track as derived from the analysis with the available empirical criteria for allowable vehicle loads, which is discussed in Section 3. The Prud'homme, 85 percent Prud'homme, Amans and Sauvage and the recent 0.5 times axle vertical load (9) are candidates for the comparison. The theoretical values used here are of course for specific track parameters, whereas the empirical criteria are supposed to be applicable for all tracks and conditions. Also the calculated static limit load is at best permissible for a stationary load application, whereas the empirical criteria are for a large number of moving load passes.

The relationship between the lateral load limit and the degree of track curvature is shown for all of the above criteria in Figure 5-14. Results of the analysis procedure discussed in subsection 5.2.3 are shown in the heavy solid lines for three different temperature levels. These temperatures represent the difference between the current rail temperature and the rail neutral (zero force) temperature. The highest level (75°F) is considered to be a realistic worst

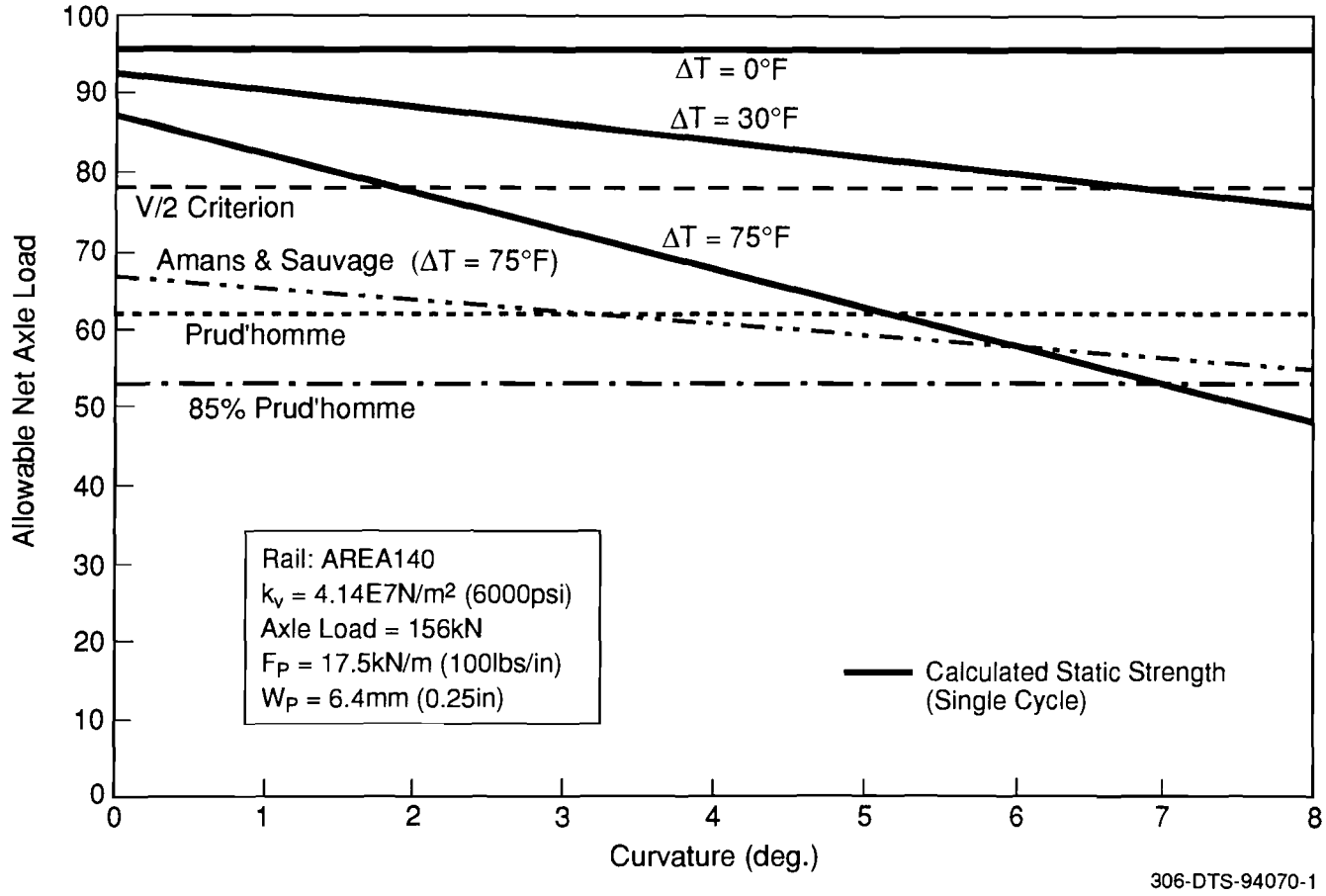

Figure 5-14. Comparison of calculated track static strength against permissible dynamic (moving) loads from empirical criteria

case. Since the limiting strength of curved tracks reduces with rail temperature increase, the criteria should include the temperature and curvature effects. Clearly the permissible loads according to any criterion should always be much lower than the static track strength for the track to withstand a number of vehicle passes. Thus, the SNCF criteria (Amans & Sauvage, and Prud'homme) seem to be more appropriate than the V/2 criterion. Their allowable loads are substantially below the static strength, thus potentially letting the track withstand many axle passes at these load levels.

5.2.5 Cumulative Residual Deflection Model

Although the analysis presented in the previous section gives some sort of an upper bound for track strength, it does not address the track shift problem in a rigorous manner. For track shift analysis, it is important to simulate moving loads and determine the stable and progressive regimes of track shift as presented in Section 2. A rigorous track shift model is currently under development. The following represent a hierarchy of problems under investigation.

- One cycle stationary load with unloading.
- Cyclic stationary loads.
- Single moving load (axle).
- Moving load under many axle passes.
- Moving truck loads under many passes.

The first three problems form building blocks in the final analysis of the track shift, ϕ, as defined by the last two problems. A basic approach for cyclic loads is presented here.

Referring to Figure 5-15 the track is unloaded at the point 1. The strain energy in deflected rails (and possibly in elastic fasteners) tends to return the track panel to its original position, but the static lateral resistance opposes it. The resulting residual deflection calculation Δ_1 can be based on the beam theory discussed above and on the static resistance data and treating the deflection w_1 as the initial imperfection, w_o. Using Δ_1 as the initial deflection, the response up to point 2 is determined. The Δ_2 is next evaluated and so on for subsequent cycles. *With increasing deflection the tie resistance available may reduce which must be properly accounted for in the analysis.*

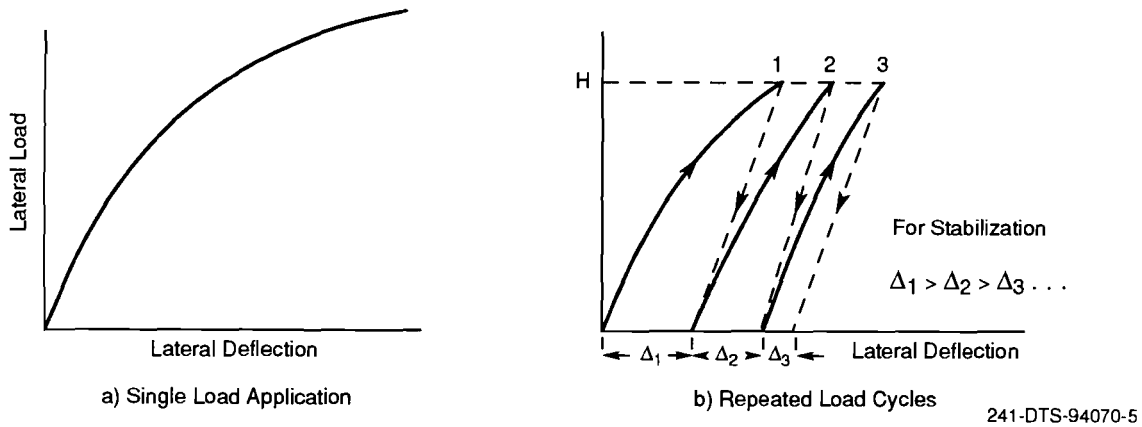

Figure 5-15. Track panel lateral response

If after a finite number of passes, the increment Δ_n becomes negligible, then the track shift is stabilized at $\Sigma\Delta_n$. On the other hand, if $\Delta_1 < \Delta_2 < \Delta_3$, the track shift occurs in rapid progression without reaching any stable limit. Such a condition has been used by the SNCF in their test data reduction. The model for the residual deflection evaluation is critical in understanding and quantifying the track shift phenomenon and requires further research.

5.3 Test Requirements

Both static and dynamic (moving load) tests will be required to assess track shift in the field conditions. Tests will also be required to evaluate the basic parameters of the track for use as inputs in the analytic models referred to in subsection 5.2.

5.3.1 Parameter Evaluation

Track parameters quantified in the United States previously are for the wood tie track with cut spike construction. Modern high speed track is unlikely to be of this construction. Assuming the modern high speed track in the United States uses concrete ties and appropriate fasteners, we will need to evaluate the following parameters for such a track.

- Tie-ballast lateral resistance (loaded and unloaded).
- Fastener torsional resistance.
- Track vertical modulus.
- Rail section properties (including flexure rigidities in vertical and lateral planes).
- CWR neutral temperature.

Test methodology to determine tie-ballast resistance has been developed in the United States. The loaded tie resistance requires simulation of large loads. (Approximately 30 percent of the axle load may be borne on the tie directly underneath the wheels.) Since test simulation of large loads on a single tie and pulling it laterally can be very cumbersome, an indirect means such as the one presented in the following subsection will be required.

Both loaded and unloaded tie-ballast resistance should be accurately measured at incremental displacement of 0.02 in. (0.5 mm) up to 1.2 to 1.6 in. (30 to 40 mm) for the track shift evaluation studies.

5.3.2 Track Panel Tests

Static loaded concrete tie track panel tests are needed to immediately accomplish the following objectives. Vehicles with two axle trucks can be conveniently used in the load simulation. Alternately the Track Loading Vehicle of AAR may be modified to simulate the single axle loads. The track panel test objectives are:

1. Determine the vertical load distributions under the vehicle load.
2. Determine the lateral load distributions under a single lateral load and the combination of lateral and vertical loads.
3. Determine the tie ballast loaded resistance as a function of the vertical load, using the data collected from (1) and (2).

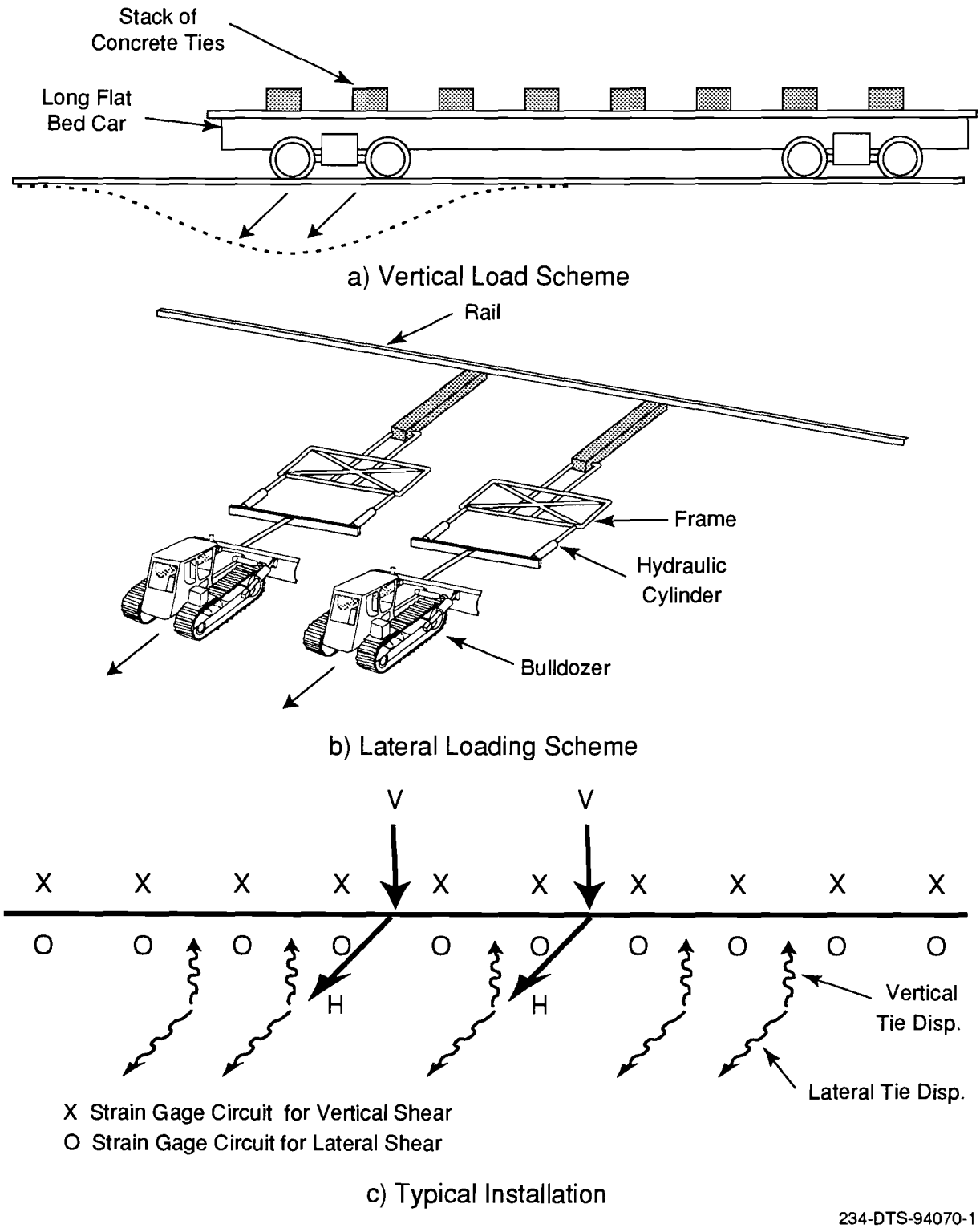

Figure 5-16. Testing and instrumentation scheme

4. Validate the analytic model for the lateral track response.

5. For cyclic loading and unloading, validate the hierarchial cumulative residual deflection models to be developed as discussed in subsection 5.2.5.

Test Methodology

The test methodology is similar to that of the Track Lateral Pull Tests (TLPT) previously conducted by VNTSC (20), except that the rails are now to be instrumented by strain gages to record the lateral and vertical shear loads, and hence the tie loads. Figure 5-16 shows the instrumentation schematically. The load deflection response is to be recorded on an x-y plotter.

The application of required vertical load can be facilitated using an appropriately loaded long flat car. The lateral load can be applied using two or more hydraulic cylinders in parallel operated by electric pumps, and reacted by two or more bulldozers. If more than two cylinders are used, the load application can be done through a "whiffle tree" arrangement.

Unloading can be done by first releasing the lateral hydraulic power and rolling the car out of the test zone. The residual deflection can be measured and the loading cycle repeated. In this setup, the vertical and the lateral loads are not truly in "phase," but this is not likely to contribute to significant error in the test results. Clearly, the track panel response for residual deflections should be performed under combinations of vertical and lateral loads covering the practical range of interest.

5.4 Summary

- Analytic models for the loaded track panel structural response in the small deflection range are critical for understanding the track shift phenomenon. Determination of 1) the vertical load distribution, 2) the lateral resistance or stiffness distribution, 3) the track lateral response under axle lateral loads, and 4) the residual deflection after the wheel passage are important parts of the required analysis. The first three parts are conceptually simpler than the last to formulate, but are mathematically involved. The determination of residual deflection is extremely complex but critical to the track shift studies.

- An approach is presented to resolve the analytic problems. Preliminary calculations on the limiting lateral load for the elastic response of the track panel under a vertical wheel load have yielded good results comparable to those of the SNCF. These calculations demonstrate the importance of the track parameters such as the tie ballast friction coefficient, peak ballast resistance, foundation modulus, rail force, and track curvature.

- Several issues which remain to be addressed are: single axle versus truck loads; stationary loads versus moving loads; and quasi-static versus time varying loads. The ballast resistance in the vibratory environment due to high speed trains should also be examined.

- Certain basic field tests may need to be performed to support the development of the analytic methods. The tests will evaluate the fundamental track parameters including the resistance within the small deflection range (<20 mm). In addition, the loaded track panel lateral response under single and repeated loads will also need to be evaluated. A test procedure is outlined that uses stationary loads for this purpose. This is relatively inexpensive and will aid the preliminary model validation. Full-scale high speed tests can be defined and undertaken after the simpler proposed test.

6. CONCLUSIONS AND RECOMMENDATIONS

6.1 Conclusions

1. Critical track shift conditions are identified in terms of cumulative residual track deflections, vehicle lateral loads, and the limiting track strength. Failure modes arising from the track shift include sudden track panel movement, derailment due to wheel climb or gage widening, and ride quality deterioration.

2. Vehicle qualification and other tests on high speed vehicles such as TGV, ICE and X2000 have been performed in Europe and recently in the United States. These tests typically evaluated the limiting vehicle speeds and loads from considerations of ride quality, wheel climb derailment and track shift. Only the SNCF performed systematic experimental studies on their TGV, which included the evaluation of allowable lateral loads from the track shift point of view. It is extremely important to evaluate the required track strength to assure that it is the basis for determining the ultimate safe vehicle speed. Although the ride quality and wheel climb considerations determine speed limits at present, modern high speed vehicles are continuously evolving to overcome these limitations through use of tilting bodies, radially steered trucks and other means.

3. Although the Prud'homme limit and other criteria are in usage for the vehicle qualification loads, the criteria, being empirical, cannot cover the wide range of track conditions that can exist. The criteria can be in some cases conservative and in some others nonconservative. Hence, a rational method of evaluating the vehicle qualification loads will be useful for safety and optimum utilization of high speed train operations. Such a method requires rigorous track shift analysis supplemented by limited well planned experiments.

4. Vehicle dynamic modeling will be an integral part of track shift studies. All the theoretical and experimental studies to date were performed for constant lateral axle loads. Vehicle dynamic models can determine dynamic loads due to hunting and misalignment negotiation. Using the SYSSIM computer simulation, the influence of track lateral misalignments has been studied; and the result shows that the peak lateral loads generated on the track can be significant at high speeds unless stringent limits on track misalignments are imposed.

5. Modeling requirements of the track structure have been identified. Determination of the track vertical response, resulting track lateral resistance distribution and the track lateral response are important in the track shift studies. Analytic methods have been suggested and demonstrated with numerical results for the lateral limiting static strength of loaded track panel. The analysis accounts for the wheel vertical load influence on the track lateral resistance, tie-ballast friction coefficient, rail thermal force and track curvature. The general case of "nonlinear" track response is involved from a numerical solution point of view, though conceptually not difficult for the differential equation formulation. The most difficult, but important, analytic task is the evaluation of the lateral residual deflection under repeated loading and unloading cycles. An approach is indicated for further consideration. Track profile degradation under repeated vertical loads is also important although this has not been discussed in this report. Similarly environmental effects (frost

heave, water flooding) are also important considerations for integrity of the track structure, but are not discussed in this report.

6. Tests on loaded track panels to determine the important track parameters and to validate the static models referred to in item 5 have been identified. Repeated loads can also be simulated in the test setup to evaluate the residual deflection.

6.2 Recommendations

1. *Static Continuum Model* - The track vertical response and the lateral resistance model are reasonably well developed. The loaded track static lateral response calculation up to its limit, as formulated in this report, seems to be reasonable. The method should be extended and numerically demonstrated for moving loads. Both single axle and truck loads should be studied. The method should account for rail temperature and curvature and any unbalanced force due to cant deficiency. The model should be extended to include repeated loads. The residual deflection at each load cycle should be determined through a proper idealization of the tie-ballast resistance.

2. *Track Dynamic Model* - A generalized track dynamic model should be developed to study the influence of quasi static moving and dynamic loads (as determined by the present SYSSIM model). The track lateral deflections should be compared with one another and with the deflections obtained from the static load idealization in item 1. The track dynamic model will resolve issues related to proper load characterization and will also provide a useful building block in the integrated vehicle-track model.

3. *Vehicle Dynamic Model* - The present vehicle dynamic model (SYSSIM) though satisfactory as used in this report, can be improved with new connections for more accurate calculations of the vehicle loads. Consideration should be given to combining the improved vehicle dynamic model and the generalized track dynamic model. Such a model will evaluate the vehicle loads and the derailment potential more rigorously than the existing vehicle dynamic model, which is connected to the track by a simplistic spring. Development of such an integrated model will be involved. Hence, it is also necessary to pursue the static continuum model in parallel to obtain solutions without undue labor for practical applications.

4. *Testing* - Static tests on instrumented loaded track panels should be performed for the determination of the tie-ballast friction coefficient at various vertical load levels, and also to validate the track lateral response model presented in this report. The panel elastic response load limit should also be determined from the tests. Repeated lateral load cases should also be studied to evaluate the growth of the residual lateral deflection with load cycles.

APPENDIX A

TRACK PANEL VERTICAL RESPONSE

Referring to Figure 5-2 which shows the structural model, the differential equation for region 2 is

$$EI_v v_2'''' + k_v v_2 = Q \tag{A-1}$$

Here, k_v is the vertical stiffness and Q is the self weight of the track/unit length.

Solution of this equation satisfying the requirement $v_2 = v_2 = o$ as $x \to \infty$ is

$$v_2 = \frac{Q}{k_v} + e^{-\xi a}(C_1 \cos \xi a + C_2 \sin \xi a) \tag{A-2}$$

where $\xi = x - s$ (see Figure 5-2) for convenience. C_1 and C_2 are integration constants, and

$$a = \sqrt[4]{k_v / EI_v}$$

The differential equation in region 1 can be shown to be

$$EI_v v_1'''' = \frac{V}{2}\delta^*(o) + Q - G_o - \overline{G}(v_1) \tag{A-3}$$

Here, V is the vertical axle load, G_o is constant and $\overline{G}(v_1)$ is the nonlinear load-deflection function, and $\delta^*(o)$ is the Dirac's delta function. G_o represents the load at the transition point between the linear and nonlinear regimes of the tie vertical response. The factor of one-half is due to the right side region ($o < x < s$) under consideration.

Note that the thermal load and fastener torsional stiffness are not included in the foregoing differential equations, as the anticipated vertical deflections are small. However, it is not difficult to include the rail force (as shown in the previous analysis), which may be required for the case of very soft foundation or large initial vertical misalignment.

Solution of Equation (A-3) will be written as

$$v_1 = C_3 + C_4 x^2 + \sum_{1,3,5}^{\infty} A_m \cos \frac{m\pi x}{2s} \tag{A-4}$$

The first two terms represent the symmetric homogeneous solutions of Equation (A-3) and the last Fourier expression is intended to satisfy the complete differential equation.

The symmetric boundary conditions at x = o are satisfied. The conditions of continuity between the two regions are

At x = s

$$v_1 = o \tag{A-5}$$

Deflection

$$v_2 = \overline{v} \tag{A-6}$$

Where $\bar{v}$ represents the matching displacement between the linear and nonlinear regimes of the ballast vertical stiffness characteristic.

Slope $v_1' = v_2'$ (A-7)

Moment $v_1'' = v_2''$ (A-8)

Shear force $v_1''' = v_2'''$ (A-9)

Defining

$$G_o - \frac{V}{2}\delta(o) - Q = \sum a_m \cos\frac{m\pi x}{2s} \tag{A-10}$$

$$\bar{G}(v_1) = \sum B_m \cos\frac{m\pi x}{2s} \tag{A-11}$$

we find from Fourier analysis

$$a_m = \frac{2}{s}\int_o^s \left[G_o - \frac{V}{2}\delta(o) - Q\right]\cos\left(\frac{m\pi x}{2s}\right)dx \tag{A-12}$$

$$= -4\, m\pi \bullet \sin\left(\frac{m\pi}{2}\right) \bullet (G_o - Q) - \frac{V}{s}$$

$$B_m = \frac{2}{s}\int_o^s \bar{G}(v_1)\cos\frac{m\pi x}{2s}\,dx \tag{A-13}$$

$$A_m = -(a_m + B_m)\Big/\left(\frac{m\pi x}{2s}\right)^4 \tag{A-14}$$

For a given value of V, there are six unknowns in the solution presented above {C_1, . . . , C_4, [A_m], s}. There are six equations (A-5) to (A-9) and Equation (A-14). Hence, a complete rigorous solution is obtained. It is convenient to treat V as the unknown for an assumed value of s. This will result into linear equations that can be easily solved. Once $v(x) = v_1(x) + v_2(x)$ is known, then the tie vertical force distribution, $R_V(x)$ is obtained from.

$$R_V(x) = k_V v(x) + Q$$

APPENDIX B

TRACK PANEL LATERAL RESPONSE

Referring to Figure 5-7, the differential equation *for region I* is

$$EIw_1'''' + P_o w_1'' = H\delta(o) - P_o w_o'' - F_{p,d} - \overline{F} \qquad \text{(B-1)}$$

Here the primes denote the derivatives with respect to x

w_1	=	deflection in region 1
P_o	=	thermal load = $AE\alpha T$ (for small deflection)
T	=	temperature rise over the neutral
A	=	cross-sectional area (two rails)
E	=	Young's modulus of rail steel
w_o	=	preexisting misalignment, if any
$F_{p,d}$	=	peak dynamic (load) resistance of tie
$\overline{F}$	=	nonlinear part accounting for softening
	=	0 (for tamped track)
H	=	lateral axle load
$\delta(o)$	=	Dirac's delta function

For region II, the differential equation is

$$EIw_2'''' + P_o w_2'' + kw_2 = o \qquad \text{(B-2)}$$

where

k	=	variable linear stiffness
	=	$F_{p,d}/w_p$
	=	$(F_{p,s} + \mu_f R_v)/w_p$

Here

$F_{p,s}$	=	peak value of static lateral resistance
μ_f	=	tie-ballast friction coefficient

Clearly, k can be written as

$$k = k_s + k_d \qquad \text{(B-3)}$$

where

k_s	=	static stiffness = $F_{p,s}/w_p$
k_d	=	additional stiffness due to vertical loading
	=	$\mu_f R_v/w_p$

Special Case $w_2 \leq w_p$

For $w_2 \leq w_p$, the inelastic track deflection, region I is not developed. The differential equation for w_2 in the right half of the region ($o < x < L$) is

$$EIw_2'''' + P_o w_2'' + kw_2 = \frac{H}{2}\delta(o) \qquad \text{(B-4)}$$

The boundary conditions on w_2 are

$$\text{At } x = L: \quad w_2 = w_2' = w_2'' = 0 \tag{B-5}$$

These conditions can be proved through the variational principle.

A solution of Equation (B-4) is developed using the Fourier method. Let

$$w_2 = \sum_{1,3,5}^{\infty} A_m \cos^{m\pi x} / 2L \tag{B-6}$$

$$k = a_o + \sum_{1,3,5} a_n \cos\frac{n\pi x}{2L} \tag{B-7}$$

Here

$$a_n = \frac{2}{L}\int_0^L \frac{\mu_f R_v}{w_p}\cos(n\pi x / L)dx \tag{B-8}$$

Substitution of the above expressions in Equation (B-4) gives

$$\sum A_m\left[EI(m\pi / 2L)^4 - P_o(m\pi / 2L)^2 + a_o\right]\cos(m\pi x / 2L)$$

$$+\sum_{\substack{m \\ 1,3,5}} \sum_{n=1,3,5} A_m\, a_n \cos\frac{m\pi x}{2L} \bullet \cos\frac{n\pi x}{2L} = \frac{H}{2}\delta(o) \tag{B-9}$$

After taking the Fourier transform of the above expression we obtain

$$\psi_i A_i + \sum_m \varepsilon_{mi}\, A_m = H / L \quad (i = 1,3,5,\ldots) \tag{B-10}$$

where

$$\varepsilon_{mi} = \frac{\Sigma a_n}{2\pi}\left\{\frac{\sin(m-n-i)\pi/2}{m-n-i} + \frac{\sin(m-n+i)\pi/2}{m-n+i}\right.$$

$$\left. + \frac{\sin(m+n-i)\pi/2}{m+n-i} + \frac{\sin(m+n+i)\pi/2}{m+n+i}\right\} \tag{B-11}$$

and

$$\psi_i = EI\left(\frac{i\pi}{2L}\right)^4 - P_o\left(\frac{i\pi}{2L}\right)^2 + a_o \qquad \text{(B-12)}$$

All the boundary conditions are satisfied, except the transversality condition at x = L which gives

$$\sum_m A_m \, m\sin\frac{m\pi}{2} = 0 \qquad \text{(B-13)}$$

This last equation together with the expression (B-10) will determine the Fourier coefficients $\{A_m\}$ and the wavelength L for a given value of H. The deflection response of H versus w can be determined. The infinite series can be truncated at a finite number of terms (usually five harmonics) due to the fast convergence of the Fourier series.

REFERENCES

1. Prud'homme, A., "Resistance of the Track to Lateral Loads Exerted by Rolling Stock," *Revue Générale des Chemins de Fer*, January 1967.

2. Amans, F. and R. Sauvage, "Railway Track Stability in Relation to Transverse Stresses Exerted by Rolling Stock. A Theoretical Study of Track Behavior," Bulletin of the International Railway Congress Association, January 1969.

3. Kish, A. and W. Mui, "A Brief Synopsis on the Track Lateral Shift Problem," American Railway Engineering Association Bulletin, No. 746, May 1994.

4. Frederick, C.O., "The Effect of Lateral Loads on Track Movement," British Railways Board, Research and Development Division, Technical Note T.1, July 1975.

5. "Study of the Lateral Resistance of Loaded Track and Determination of its Lateral Resistance Limit," SNCF report, E.1210-80-06, May-June 1980.

6. "Evaluation of the Lateral Resistance of the Loaded Track from Static Tests," DT 150 (C 138), Office for Research and Experiments of the International Union of Railways (ORE), January 1986.

7. "Measurements of the Lateral Strength of the Track," SNCF Draft Report E. 1210 - 91 - 02, June 1991.

8. "Measurement of Track Displacement Force on Different Types of Track," Internal Report IR-90-XX, November 1990.

9. Whitten, B.T., and B.T. Scales, "X2000 U.S. Demonstration, Vehicle Dynamics Tests, Final Test Report," DOT/FRA/ORD-94/15, Nov. 1993.

10. "Railroad Passenger Safety," DOT/FRA/ORD-89/06, April 1989.

11. Cervi, G., "High Speed Rail Track Structure Design and Maintenance," Transportation Research Board, Annual Congress, January 1994.

12. Bourdon, Y., A. LeBihan, and D. Bourdon, "European Rail for High-Speed Tracks," Transportation Research Board, Annual Congress 1994.

13. Bijl, F., "The Horizontal Buckling of Long Welded Tracks," ORE Document DTS, Utrecht, 1958.

14. Private communication from British Rail to G. Samavedam.

15. Tanabe, M. "Dynamic Interaction Analysis Model of Shinkansen Vehicles, Rails and Structures," Proceedings of the International Conference on Speedup Technology for Railway and Maglev Vehicles, Vol. 2, Nov, 22-26, 1993.

16. Kondoh, K., "New Way of Track Maintenance on High Speed Railway - Development of Automatic Mechanized Track Lining System (AMTLS)," Proceedings of the International Conference on Speedup Technology for Railway and Maglev Vehicles, Vol. 1, Nov, 22-26, 1993.

17. Pospischil, R., Effects of a Modified Type of Superstructure, Chapter 3, *"Quantitative Marginal Conditions for the Track Parameters and Their Limit Values."*

18. Luebke, D., "Vehicle/Track System Behavior," Proceedings of the International Conference on Speedup Technology for Railway and Maglev Vehicles, Vol. 1, Nov, 22-26, 1993.

19. Whitten, B., K. Kessler, and D. Stout, "Quick Look Data Summaries, Limiting Conditions from the Amtrak ICE Test," Unpublished Preliminary Data Report, July 1993.

20. Samavedam, G., A. Kanaan, J. Pietrak, A. Kish, and A. Sluz, "Wood Tie Track Resistance Characterization and Correlations Study," DOT/FRA/ORD - 94/07, 1994.

21. Samavedam, G., A. Kish, A. Purple, and J. Schoengart, "Parametric Analysis and Safety Concepts of CWR Track Buckling," DOT/FRA/ORD-93/26, December 1993.

22. "Safety Relevant Observations on the ICE High Speed Train," DOT/FRA, July 1991.

23. "Safety Relevant Observations on the TGV High Speed Train," DOT/FRA, July 1991.

24. Blader, F.B., "Assessing Proximity to Derailment from Wheel/Rail Forces: A Review of the State of the Art," RTD-Vol.3, Rail Transportation, ASME, 1989.

25. Eickhoff, Bridget M., "Assessment of Passenger Reaction to Vehicle Ride," RTD-Vol.6, Rail Transportation, ASME, 1993.

26. Casini, C., R. Cheli, and G. Piro, "ETR 500 and ETR 450/460 High Speed Trains of Italian State Railways - Main Features and Test Results," Proceedings of the International Conference on Speedup Technology for Railway and Maglev Vehicles, Vol. 1, Nov, 22-26, 1993.